

Electronic Thesis and Dissertation Repository

9-14-2018 2:00 PM

The Effect of Seizures (Afterdischarges) on Hippocampal Long-Term Potentiation

Vishaka Rajan, *The University of Western Ontario*

Supervisor: Leung, Stan, *The University of Western Ontario*

A thesis submitted in partial fulfillment of the requirements for the Master of Science degree in Neuroscience

© Vishaka Rajan 2018

Follow this and additional works at: <https://ir.lib.uwo.ca/etd>



Part of the [Neuroscience and Neurobiology Commons](#)

Recommended Citation

Rajan, Vishaka, "The Effect of Seizures (Afterdischarges) on Hippocampal Long-Term Potentiation" (2018). *Electronic Thesis and Dissertation Repository*. 5694.
<https://ir.lib.uwo.ca/etd/5694>

This Dissertation/Thesis is brought to you for free and open access by Scholarship@Western. It has been accepted for inclusion in Electronic Thesis and Dissertation Repository by an authorized administrator of Scholarship@Western. For more information, please contact wlsadmin@uwo.ca.

ABSTRACT

This study investigated whether an electrographic seizure, or an afterdischarge (AD), inhibits long-term potentiation (LTP) in the hippocampus. Neuromodulation by acetylcholine (ACh) and genetic modification by loss of the ATRX gene on LTP was also examined through the use of VAChT knockout mice and ATRX knockout mice, respectively. Evoked potentials were recorded in the hippocampal CA1 region in freely behaving mice and urethane-anesthetized mice. Basal dendritic LTP was suppressed when elicited 1 h after an AD in all behaving mice, regardless of mouse genotype; LTP was unaffected when induced 1 day or 1 week following an AD. At 1 h post-AD, LTP suppression was largest at <30 min after theta-frequency burst stimulation (TBS). In the urethane-anesthetized mice, no significant LTP was elicited at 1 h after an AD of 4.5 – 15 s duration, compared to when no AD was evoked irrespective of mouse genotype. In addition, postictal response and LTP magnitude were both negatively correlated with AD duration. Thus, this study has demonstrated that LTP can be suppressed by an AD that was induced one hour earlier, with AD duration being an important factor that contributes to this suppression effect.

Keywords: synaptic plasticity; hippocampus; memory formation; afterdischarge; CA1; mice; current source density

STATEMENT OF CO-AUTHORSHIP

I hereby declare that this thesis incorporates material that is result of joint research, as follows:
Chapter 2 of the thesis was co-authored with Liangwei Chu and Radu Gugustea, under the supervision of Dr. Stan Leung. Liangwei Chu and Radu Gugustea contributed to the surgical procedures of the chronic and acute mice paradigms, respectively. In all cases, the key ideas, primary contributions, data analysis, interpretation, and writing were performed by the author.

ACKNOWLEDGEMENTS

I would like to thank to everyone who has supported me throughout my graduate school experience and with this project. First, I would like to thank my supervisor, Dr. Stan Leung, whose guidance has been paramount to my growth as an individual and a researcher. It has been my privilege to work with a leading expert in the field of electrophysiology. I would also like express my gratitude to the members of my lab who have helped me with my project. I am especially grateful for Liangwei Chu and Radu Gugustea for teaching me a wide range of technical skills and providing me with the resources necessary to complete my project. A special thank you to Thyna Vu for all of her advice and support. I would also like to thank my advisory committee members, Dr. Michael Poulter and Dr. Brian Allman, for their advice and encouragement throughout the course of this project. Lastly, I would like to thank my family and friends for their continual support throughout this incredible academic journey.

TABLE OF CONTENTS

ABSTRACT AND KEYWORDS	i
STATEMENT OF CO-AUTHORSHIP	ii
ACKNOWLEDGEMENTS	iii
TABLE OF CONTENTS	iv
LIST OF FIGURES AND TABLES	vi
LIST OF ABBREVIATIONS AND NOMENCLATURE	viii
1. Introduction.....	2
1.1 Hippocampal anatomy.....	2
1.2 Learning and memory in the hippocampus.....	5
1.3 Long-term potentiation.....	6
1.3.1 Paired-pulse facilitation.....	11
1.3.2 Neuromodulation of LTP.....	11
1.4 Temporal lobe epilepsy.....	12
1.5 Afterdischarges: formations and mechanism.....	12
1.5.1 Effect of afterdischarges on behaviour.....	14
1.5.2 Afterdischarges and LTP.....	15
1.6 Extracellular field potentials.....	16
1.7 Rationale	17
1.7.1 Aim 1	18
1.7.2 Aim 2	18
1.7.3 Aim 3	18
2. METHODS	19
2.1 Animals for chronic recording.....	19
2.2 Electrode implantation	19
2.3 Experimental procedure.....	20
2.3.1 Session 1: LTP induced by theta-frequency burst stimulation (TBS).....	21
2.3.2 Session 2: AD followed 1h by TBS.....	22
2.3.3 Session 3: TBS alone.....	23
2.3.4 Session 4 and 5: AD followed 1 day by TBS.....	23
2.4 Perfusion	24
2.5 Histology and Staining.....	25
2.6 Statistical Analysis	25
2.7 Animals for acute recording.....	27
2.8 Electrode implantation	27
2.9 Surgery.....	27
2.10 Acute experimental procedure.....	28
2.11 Perfusion	31
2.12 Histology and Staining.....	31
2.13 Statistical analysis	31
3. RESULTS	33
3.1 LTP induced by theta-frequency burst stimulation (TBS).....	33
3.2 AD followed 1h by TBS	36
3.2.1 AD-1h LTP vs. LTP only, all mice.....	40
3.2.2 AD-1d LTP vs. LTP only, all mice.....	41
3.2.3 Postictal depression vs AD duration in behaving mice.....	42
3.2.4 LTP vs AD duration in behaving mice.....	45

3.2.5 Postictal depression vs LTP.....	46
3.3 Responses in urethane-anesthetized mice	46
3.3.1 AD duration vs LTP.....	50
3.3.2 AD duration vs postictal response.....	54
3.3.3 Postictal response vs LTP.....	57
3.3.4 Group analysis of the effect of an AD on postictal response.....	60
3.3.5 Group analysis of the effect of an AD on LTP.....	62
3.3.6 Group analysis of primed burst tetanus	64
4. DISCUSSION	65
4.1 Main results	65
4.2 AD, postictal response, and LTP in chronic behaving mice paradigm	65
4.3 AD, postictal response, and LTP in acute urethane-anesthetized mice paradigm.....	66
4.4 Previous studies on AD vs LTP.....	69
4.5 Potential mechanisms of LTP suppression by AD	70
4.6 Future studies	71
5. REFERENCES.....	73
6. APPENDIX.....	80
6.1 Ethical approval for animal use.....	80
6.2 Copyright Permission.....	81
7. CURRICULUM VITAE.....	82

LIST OF FIGURES AND TABLES

Figure

1. Schematic diagram of hippocampal connections	4
2. Evoked field potential during excitation of the basal dendrites	17
3. A coronal section of the mouse hippocampus illustrating the position of recording and stimulating electrodes for chronic experiments	20
4. Slope measurements taken from analyzed averaged evoked potentials.....	22
5. Flow chart representing timeline of experiments proposed for mice in the chronic experimental paradigm.....	24
6. Coronal slices indicating electrode location	26
7. A coronal section of the mouse hippocampus illustrating the position of recording and stimulating electrodes for acute experiments.....	28
8. Averaged evoked potentials and current source density transients in CA1 from representative mice ...	30
9. Flowchart representing timeline of experiment for all mice in the urethane-anesthetized acute paradigm.....	31
10. Slope measurements taken from CSD analyzed averaged evoked potentials.....	33
11. Representative average evoked potential traces in which TBS was applied.....	35
12. A representative experiment in which TBS was applied to the Schaffer collateral pathway	36
13. Representative average evoked potential traces in which an AD was applied	38
14. A representative experiment in which an AD was applied, followed 1 hour by TBS tetanus	39
15. A representative set of experiments of various LTP paradigms in chronic behavioural mice.....	40
16. Normalized E1 post-TBS response curves for the LTP-only and AD-1h LTP treatments.	41
17. Normalized E1 post-TBS response curves for the LTP-only and AD-1d LTP treatments	42

18. Normalized E1 post-TBS response curves for the LTP-only and AD-1w LTP treatments.....	43
19. Mean basal dendritic fEPSP slope values for all mice for both the LTP only and the AD-1h LTP treatments.....	44
20. A series of graphs depicting the relation between postictal response to AD duration.....	45
21. Linear regression analysis of mean LTP response against corresponding AD duration.....	46
22. Linear regression analysis of mean LTP response and postictal response.....	48
23. A representative experiment where an AD of 0s was evoked followed 1 hour by TBS tetanus	49
24. A representative experiment where an AD of 4.5s was evoked followed 1 hour by TBS tetanus	51
25. Electrographic activity at a CA1 distal dendritic electrode of selected experiments, before and after high-frequency stimulation	53
26. Linear regression analysis of cCA3 evoked post-TBS response at 20 min with AD duration	53
27. Linear regression analysis of iCA3 evoked post-TBS response at 20 min with AD duration	53
28. Linear regression analyses of cCA3 postictal response to AD duration.....	55
29. Linear regression analyses of iCA3 postictal response to AD duration.....	56
30. Linear regression analyses of cCA3 LTP response at (A) 10 min and (B) 20 min post-TBS with cCA3 postictal response at 60 min post-AD	58
31. Linear regression analyses of iCA3 LTP response at (A) 10 min and (B) 20 min post-TBS with iCA3 postictal response at 60 min post-AD	59
32. Postictal responses for no-AD and AD groups, showing mean and SEM of E1, E2 and E2/E1 across the duration of postictal response	61
33. Responses after theta-burst stimulation (TBS) in no-AD and AD groups, showing mean and SEM of E1, E2 and E2/E1 across all post-TBS time points.....	63
34. Group average of no-AD and AD groups, showing mean and SEM of the first pulse of TBS across all 4 traces	64

LIST OF ABBREVIATIONS

-	negative
+	positive
CAMKII	calcium/calmodulin-dependent protein kinase II
ACh	acetylcholine
AD	afterdischarge
AEP	average evoked potential
AMPA	α -amino-3-hydroxy-5-methyl-4-isoxazolepropionic acid
ANOVA	analysis of variance
ATRX	α -thalassemia X-linked mental retardation syndrome
Ca ²⁺	calcium ion
CSD	current source density
DA	dopamine
DG	dentate gyrus
EC	entorhinal cortex
fEPSP	field excitatory post synaptic potential
GABA	γ -Aminobutyric acid
HET	heterozygous (genotype)
HFS	high frequency stimulation
K ⁺	potassium ion
KD	knockdown
KO	knockout
LTP	long-term potentiation
Mg ²⁺	magnesium ion
mGluR	metabotropic glutamate receptor
Na ⁺	sodium ion
NMDA	N-methyl-D-aspartate
OR	stratum oriens
PIP	postictal potentiation
PPF	paired pulse facilitation
PYR	stratum pyramidale
RAD	radiatum- and dentate-innervating (cells)
RE	nucleus reuniens
SLM	stratum lacunosum moleculare
TBS	theta burst stimulation
VAcHT	vesicular acetylcholine transporter
VTA	ventral tegmental area

Chapter 1: Introduction

1.1 Hippocampal structure

The hippocampus, located in the medial temporal lobe, is a structure that has long been the focus of neuroscience research due to its prominent role in learning and memory. The hippocampus itself is a part of a larger group of structures known as the hippocampal formation, which consists of the subiculum, dentate gyrus, hippocampus proper, and entorhinal cortex (Johnston & Amaral, 1998). The hippocampus is a unique structure due to its organization, which is based on anatomy and function. The hippocampus proper is divided into CA3, CA2, and CA1 regions. Superimposed over the CA subregions lies the alveus, which is adjacent to the fimbria, a major input-output fiber bundle (Johnston & Amaral, 1998). The basal dendrites of the pyramidal cells lies in the stratum oriens layer, which is located between the alveus and stratum pyramidale, the layer of pyramidal cell bodies (Johnston & Amaral, 1998). Below the stratum pyramidale is the stratum radiatum, where the proximal apical dendrites can be found (Johnston & Amaral, 1998). Under the stratum radiatum is the stratum lacunosum moleculare (SLM), which contains the distal apical dendrites (Johnston & Amaral, 1998).

The hippocampus receives various sensory inputs from the neocortex via the entorhinal cortex. Through the perforant pathway, the entorhinal projections are sent to the dentate gyrus, CA3 and CA1. The dentate gyrus projects to CA3 via mossy fibres (Johnston & Amaral, 1998). CA3 projections travel via the Schaffer collateral pathway to the CA1, where they synapse onto basal and apical dendrites (Johnston & Amaral, 1998). The principal cells of the hippocampus are the pyramidal cells, found in the CA3 and CA1, and granule cells in the dentate gyrus. These cells are excitatory and use glutamate as their primary neurotransmitter. Hippocampal pyramidal cells have a triangular cell body, with basal dendrites that extend into the stratum oriens and apical dendrites

that extend into the stratum radiatum and stratum lacunosum moleculare (Johnston & Amaral, 1998). The principal cells are inhibited by interneurons that use gamma-aminobutyric acid (GABA) as an inhibitory neurotransmitter. There are various types of interneurons that can be classified based on characteristics like shape and location; these different interneurons have specified areas of innervation. The SLM has several interneurons such as apical dendrite innervating cells, basket cells, perforant path-associated interneurons, Schaffer collateral pathway-associated neurons, radiatum- and dentate-innervating (RADI) cells, oriens lacunosum-moleculare (OLM) cells, and neurogliaform cells (Capogna, 2011). The majority of work on these interneurons has been on the neurogliaform cells, which gates information between the entorhinal cortex and the CA1 in the SLM and can be blocked by a GABA_A receptor antagonist but not by a GABA_B receptor antagonist. These interneurons also fire in vivo at theta frequency, and thus may contribute to the generation of theta rhythm in the hippocampus (Capogna, 2011). OLM cells have also been shown to inhibit distal dendrites of CA1 pyramidal cells while disinhibiting proximal dendrites (Leão et al., 2012).

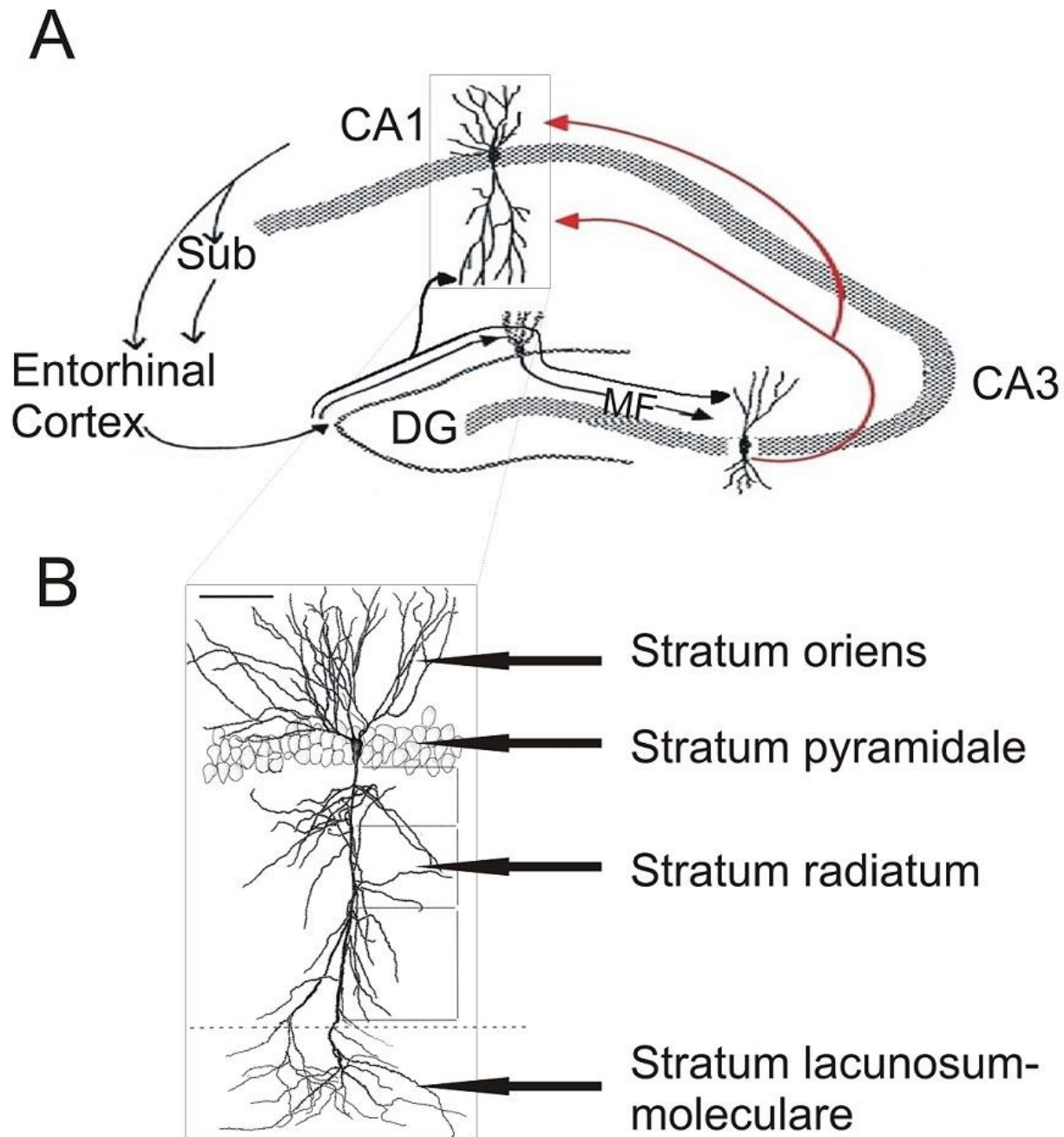


Fig 1.1. Schematic diagram of hippocampal connections. (A) Coronal section of a rat hippocampus depicting major subregions and circuitry. Arrows indicate direction of information propagation. Information enters the entorhinal cortex from the neocortex and projects directly to CA1 or projects through trisynaptic circuit by first synapsing on the DG. DG projects to CA3 via mossy fiber pathway and the CA3 then projects to the CA1 via the Schaffer collateral pathway. Information leaves from the CA1 to the entorhinal cortex. (B) Organization of different layers in CA1 of the pyramidal cells. Basal dendrites are located in the stratum oriens, proximal apical dendrites are found in the stratum radiatum, and distal apical dendrites are in the stratum lacunosum moleculare (originally illustrated by (Megias et al., 2001), reproduced with permission).

1.2 Learning and Memory in the Hippocampus

The hippocampus is widely known for its importance in memory and learning processes, with a large focus on episodic and spatial memory. This former type of memory is considered declarative memory, as it references specific events from one's experiences. Evidence of the association between the hippocampus and episodic memory has been demonstrated in patients that have had lesions in this brain region, with the most famous study being of patient H.M. As a part of a surgery meant to relieve him of his epileptic seizures, H.M. had bilateral damage to the hippocampus, entorhinal cortex, perirhinal cortex, and parahippocampal cortices (Augustinack et al., 2014). After the surgery, it was discovered that his ability to form new episodic memories was impaired. However, learning in hand-eye coordination tasks was still possible, despite H.M. claiming not to remember ever performing the task (Augustinack et al., 2014). The inability to consolidate and retrieve new information gave strong indication that pathways within the medial temporal lobe are necessary for establishing declarative long-term memory (Augustinack et al., 2014; Scoville and Milner, 1957).

The connection between the hippocampus and spatial memory was spurred by the discovery of hippocampal place cells in rats, which fire when an animal is in a specific place in an environment, thereby making them location-specific (O'Keefe, 1979). Lesions of the hippocampus resulted in impaired performance on tasks that required utilization of spatial memory, indicating that the hippocampus is involved in either the processing or retrieval of spatial information (Jarrard, 1993). While it has been established that the hippocampus is an important structure in learning and memory processes, its role in encoding, consolidation, and retrieval remains unclear.

1.3 Long-term Potentiation

While the storage of memory can be assessed behaviourally, observing the physiological mechanism behind the process has been more of a challenge. Various theories have been posited regarding the way the brain processes and stores memory. Donald Hebb (1949) suggested that learning and memory occurs as a result of association between different neurons. If two neurons were activated at the same time, the association between the firing of these two neurons would be strengthened. This strengthening of the neuronal synaptic firing would in essence form the neural basis for memory.

Long-term potentiation (LTP) is considered one of the major models of synaptic plasticity. Essentially, it is a long-lasting strengthening of synaptic transmission that results from repeated activation of synapses (Bliss & Collingridge, 1993). LTP is also synapse-specific: only synapses receiving both pre- and postsynaptic stimulation will express changes in synaptic response. Based on this mechanism, the phenomenon of LTP is linked to Hebb's theory of learning and memory.

LTP is characterized by several basic features including input specificity, associativity, cooperativity and temporal persistence. Being input-specific, LTP only occurs along the pathways that are stimulated with tetanus; non-activated pathways do not show LTP (Bi & Poo, 2001; Wigström & Gustafsson, 1986). Associativity in LTP is seen in the potentiation of weak inputs when paired with a convergent strong input. In terms of cooperativity, LTP of a weak input cannot be induced without a tetanic boost strong enough to meet threshold levels of stimulation. Finally, temporal persistence is expressed as the presence of LTP over a period of several hours following tetanic stimulation, or even several days to months in *in vivo* experiments (Abraham & Williams, 2003). LTP's temporal persistence and input-specificity make it a logical neural correlate to learning, as memories also last over long periods of time and are specific and separate from one

another. The inability to induce hippocampal LTP has been shown to impair acquisition and retention of spatial learning (Morris et al., 1986).

Initially, LTP was induced through high-frequency stimulation (HFS) trains, e.g., 100 pulses were given at 100 Hz in the span of 1 s. However, this does not reproduce hippocampal firing pattern under normal physiological conditions. The theta-burst stimulation (TBS) pattern depicts a more physiologically-relevant method; typically, neurons fire in short bursts with a burst interval in the theta range (3-12 Hz) (Fox & Ranck, 1975). Under this protocol, several short bursts are delivered at 5 Hz, and are successful in inducing LTP in the Schaffer collateral synapse.

When there is excitatory transmission, glutamate is released from the presynaptic vesicles. The glutamate then binds to NMDA and AMPA receptors in the postsynaptic neuron. AMPA receptors, when activated, allow for the movement of Na^+ and K^+ ions, which contributes to the excitatory postsynaptic potential (EPSP). However, NMDA receptors are needed for synaptic plasticity to occur. At rest, NMDA receptors are blocked by the presence of Mg^{2+} and require sufficient depolarization in order to expel Mg^{2+} and allow for Na^+ and Ca^{2+} to enter the cell. In the case of NMDA-dependent LTP, the Ca^{2+} influx is essential in activating various kinases, which lead to an increase in the presynaptic release of glutamate and a long-lasting increase in AMPA receptors at the post-synapse (Bliss & Collingridge, 1993). If the EPSP increases and is sustained for greater than 30 minutes without returning to baseline, it is considered LTP.

NMDA-independent LTP is another form of LTP, and appears to be dependent on voltage-gated calcium channels. Ca^{2+} appears to be essential for LTP as blocking the refilling of Ca^{2+} in intracellular stores or the increase of postsynaptic Ca^{2+} blocks LTP induction, whereas increasing postsynaptic Ca^{2+} can mimic LTP (Lynch et al., 1983). The downstream signaling effects of Ca^{2+} are mediated by α -calcium/calmodulin-dependent protein kinase II (αCaMKII); it is thought to

phosphorylate AMPA receptor subunit GluR1 and lead to an increase in the single-channel conductance of homomeric GluR1 AMPA receptors, thereby inducing LTP (Kandel et al., 2014). While phosphorylation of α CaMKII for one hour is associated with LTP induction, there is still no direct evidence that it must remain active to maintain LTP. It is also theorized that LTP is modulated by multiple other kinases including protein kinase A, however the role of these kinases is still not understood (Bliss et al., 2007).

The apical dendrites of the CA1 that receive from CA3 through the Schaffer collaterals have been the conventional site to elicit LTP in the hippocampus. However, the Schaffer collaterals also project from CA3 to basal dendritic synapses of CA1, making it another site for assessing LTP. HFS stimulation, rather than TBS, is more successful in eliciting LTP at the apical dendritic synapses, while both HFS and TBS elicited basal dendritic LTP (Leung & Shen, 1995). These findings show that the different synapses on the CA1 pyramidal cells may have unique roles in the way they encode information; the basal dendrites may be activated by theta-frequency inputs whereas the apical dendrites may be activated by inputs that are of high-frequency.

Various studies have sought to establish a causal link between LTP and memory processes. LTP itself consists of two phases: early phase LTP, which lasts 2-3 h and is independent of protein synthesis, and late phase LTP, which is more persistent; it is this latter phase that is associated with memory formation, as the production of proteins is thought to lead to synaptic remodelling necessary for the establishment of memories (Lynch, 2004). Numerous studies have shown that knockout of proteins or signalling factors necessary for LTP formation have led to impairment in memory performance, indicating that there is a relationship between this form of synaptic plasticity and memory formation processes (Lynch, 2004; Anagnostaras et al., 2002; Bach et al., 1995; Mayford et al., 1996). One of the best known studies that looks at the effects of LTP on spatial

memory is the Morris water maze task; in this task, rats are trained to use distal cues to locate the hidden platform (Morris, 2003). It was discovered that rats that had been injected with AP5, an NMDA-antagonist that blocked LTP, were unable to perform the task compared to their control counterparts, thereby indicating that NMDA-dependent LTP is required for spatial memory tasks (Morris, 2003).

Another prominent theory regarding the relationship between LTP and memory is that maximal expression of LTP or saturation can lead to deficits in learning and memory (Barnes et al., 1994). The concept stems from the hypothesis that neural networks store information through specific distribution of synaptic strengths; this distribution can be affected by LTP saturation, which produces further changes to the network (Barnes et al., 1994). Several studies have looked at this effect but with mixed results; while some have been able to show impairment in spatial memory tasks (Moser et al., 1998), others have been less successful in showing this impairment (Barnes et al., 1994; Cain et al., 1993; Jeffrey & Morris, 1993; Sutherland et al., 1993). A popular explanation for this discrepancy is that activation of only a small portion of entorhinal afferents may not be enough to lead to strong saturation effects (Moser et al., 1998). Based on the variable results, it has been postulated that LTP saturation effects are sigmoidal in nature such that deleterious effects are witnessed before the saturation point has been reached (Barnes et al., 1994; Moser et al., 1998).

In order to avoid the effects of saturation, various intercellular signalling molecules can directly regulate the degree of LTP (Abraham, 2008). However, regulation can also occur across time. Here, neural activity at one point in time can influence cells to modify their ability to exhibit LTP at another point in time; this is referred to as metaplasticity (Abraham, 2008). In essence, metaplasticity is the “plasticity of synaptic plasticity” and its key feature is that the change it triggers lasts beyond the triggering session of activity and persists until the LTP-inducing session

(Abraham, 2008). The priming stimulation does not change the synaptic strength but rather changes synaptic readiness to induce LTP later on (Abraham, 2008). Metaplasticity has been shown to be mediated by NMDA receptor activation (Abraham, 2008; Fujii et al., 1996; Huang et al., 1992; Coan et al., 1989) and protein kinase activation (Abraham, 2008; Woo & Nguyen, 2002), both of which are homosynaptic examples of metaplasticity. Heterosynaptic metaplasticity, where activity at one set of synapses can affect neighbouring synapses, has also been observed (Abraham, 2008; Abraham et al., 2001). Metaplasticity is important not only for its regulatory role with LTP, but also for its potential ability to prevent excitotoxicity (Abraham, 2008). Understanding the molecular mechanisms that govern this phenomenon and the various applications of it in learning and memory could potentially be used in clinical settings.

1.3.1 Paired-pulse facilitation

Paired-pulse facilitation (PPF) is a form of synaptic enhancement where two pulses are applied within a short interval, leading to an enlarged response following the second pulse. The most popular theory for this phenomenon is the residual calcium theory: when there is residual calcium still in the synapse when the second pulse is applied, there is an increase in calcium concentration, which leads to an increase in neurotransmitter release and a larger response. Apart from the need for residual calcium, the interval between the pulses is also important; as interpulse interval increases, the magnitude of facilitation decreases (Zucker & Regehr, 2002). PPF is commonly seen as a type of short-term synaptic plasticity that has a similar mechanism to LTP.

However, the relationship between these two forms of plasticity is unclear. While LTP is associated with presynaptic and postsynaptic changes (Maruki et al., 2001; Bliss & Lomo, 1973), PPF is primarily associated with presynaptic transmitter release (Zucker & Regehr, 2002). Various studies have attempted to determine whether LTP induction has an effect on PPF; in in-vitro

studies, it was found that there was no significant difference in average PPF between pre- and post-LTP but there were individual differences in slices showing an inverse change in initial PPF magnitude with LTP (Schulz et al., 1994; Maruki et al., 2001). While PPF seems to both increase and decrease in relation to LTP, it still provides a mechanism of indirectly examining the role of increased calcium in inducing LTP.

1.3.2 Neuromodulation of LTP

While the main neurotransmitter in the CA1 region is glutamate, it has been shown that other neurotransmitters play a key role in modulating synaptic transmission and LTP.

One such neurotransmitter is dopamine (DA). It has been suggested that the ventral tegmental area (VTA) innervates the hippocampus through dopaminergic inputs (Rossato et al., 2009). When D1/D5 dopaminergic receptors are blocked with an antagonist, it suppressed LTP facilitation, whereas applying an agonist has facilitated LTP induction, indicating that dopamine may play an important role in the induction of LTP (Li et al., 2003). Electrophysiological studies have shown that dopamine affects LTP facilitation at both the apical and basal dendrites (Navakkode et al., 2012; Sajikumar & Frey, 2004). Additionally, animal studies have shown that dopamine plays a role in memory; injection of DA antagonists into the hippocampus blocked long-term memory storage whereas injection of DA agonists led to the formation of persistent memories (Rossato et al., 2009).

Another important neurotransmitter is acetylcholine (ACh). The hippocampus receives cholinergic inputs from the medial septum. When slices of rat hippocampus were treated to carbachol, a cholinergic agonist, LTP was enhanced in the CA1 region, lending credence to the theory that ACh can affect LTP development (Blitzer et al., 1990). Similarly, electrophysiological studies have shown that ACh facilitates LTP at the basal dendrites of the CA1 (Doralp & Leung, 2008). It has

also been shown that mice completely deficient in vesicular ACh transporter (VACHT) in the forebrain had impaired LTP, indicating that cholinergic signalling is important for synaptic plasticity in the hippocampus (Al-Onaizi et al., 2016).

1.4 Temporal lobe Epilepsy

Temporal lobe epilepsy (TLE) is one of the most common forms of acquired epilepsy in adults (Tatum, 2012). At least 80% of all temporal lobe seizures arise in the hippocampus, with dysregulation of hippocampal function being the most predominant feature (Tatum, 2012). This impairment to the hippocampus is effectively the source of the difficulties in formation and storage of long-term memory that many patients face (Stretton & Thompson, 2012). Another feature of note in TLE is the presence of hippocampal paroxysmal discharges that are not associated with any behaviour changes; these nonconvulsive focal seizures, called afterdischarges, can occur spontaneously up to 60 times in an hour (Twele et al., 2017).

1.5 Afterdischarges: formation and mechanisms

An afterdischarge (AD) is described as a discharge of neural impulses following stimulation. In model animals, hippocampal ADs can be evoked through electrical stimulation of afferent pathways (Cain et al., 1993; Green & Petsche, 1961; Gloor et al., 1961; Kandel & Spencer, 1961; Somjen et al., 1985). In an AD, numerous cells discharge all at once, resulting in a large-amplitude synchronous spike as opposed to the normal asynchronous spiking of neurons (Bromfield et al., 2006). An AD is also called an electrographic seizure, which is best described as a clinical manifestation of abnormal, excessive, hypersynchronous discharges of cortical neurons (Bromfield et al., 2006).

An AD occurs in response to stimulation when depolarization across neuronal membranes is maintained via elevated levels of interstitial $[K^+]$, which activates a persistent $[Na^+]$ current across

the membrane (Kager et al., 2006). Variation in these ionic currents affects AD duration and threshold (Kager et al., 2006), but all afterdischarges end once repolarization occurs; this is due to a decrease in levels of extracellular $[K^+]$ relative to intercellular $[K^+]$. Afterdischarges may be simple or self-regenerating tonic (regular), or clonic (burstfire) and are always self-limiting (Kager et al., 2006). Tonic afterdischarges are produced when Ca^{2+} currents and Ca^{2+} -dependent K^+ currents are small or absent, with simple tonic ADs characterized by a short duration and high frequency of firing rate that gradually declined and, self-regenerating ADs characterized by a long duration with a high frequency of firing rate that was maintained (Kager et al., 2006). While various ion factors come into play, the accumulation of K^+ has been recognized as a critical player in the maintenance and shaping of an AD.

In the kindling model of epilepsy, repeated delivery of afterdischarges leads to increase in the AD duration and severity of behavioural seizures (Delgado & Sevillano, 1971; Goddard et al., 1969; Racine, 1972; Teskey et al., 1995). Similarly, repeated electrical stimulation of certain brain areas in the hippocampus has been shown to decrease the AD, and increase the AD/seizure duration and severity of motor seizures (Racine, 1972).

After an AD has been delivered, there is a period of post-seizure depression that is commonly referred to as postictal depression. In an *in vitro* model, it has been characterized as a transient depression of evoked synaptic activity lasting 5-10 min (Barr et al., 1997). Studies have found that duration of postictal depression can be correlated with duration of an AD (Barr et al., 1997; Stasheff et al., 1985). It has been shown that attempting to induce LTP during this period of postictal depression is unsuccessful, showing that synaptic plasticity is impaired after an ictal event (Barr et al., 1997). This could potentially explain seizure-induced amnesia that is seen in epilepsy (Barr et al., 1997; Halgren & Wilson, 1985).

1.5.1 Effect of afterdischarges on behaviour

Elucidating the effect of ADs on behaviour has remained a challenge. Cain et al. (1993) discovered that mice with AD appeared to be impaired in place-learning tasks, likely a result of the ADs induced. Conversely, Coleshill et al. (2004) discovered that electrical stimulation of the hippocampus in humans, below the AD threshold, led to deficits in word (left hippocampus) and face memory (right hippocampus); similar results were obtained by Jacobs et al. (2016) while examining the effects of deep-brain stimulation on the hippocampus. Therefore, one could infer that inducing ADs could have a greater impact on recognition memory. Indeed, ADs (or partially, subclinical seizures) in the medial temporal lobe (MTL) were suggested to result in amnesia and recent memory deficits, albeit with a small sample size (Halgren & Wilson, 1985). Coleshill et al. (2004) also noted that previous studies involving AD and memory by Halgren et al. (1978; a, b) and Halgren & Wilson (1985) were subjected to issues regarding the spreading of ADs once induced, which prevented them from isolating disruption of memory function due to electric stimulation. As such, determining the effects of an AD on memory remains elusive.

A single seizure can have profound physiological and neurological effects, such as hyperlocomotion, sensorimotor gating deficits (Ma et al., 1996; Leung, 2017). Cain et al. (1993) demonstrated that within an hour following a kindled seizure in rats, elevated escape times were found to reach a hidden platform in the water maze. Similarly, Teskey et al. (2008) showed that seizure-induced motor map expansion in the rat neocortex, and resulted in more errors in forelimb movement and during the rung walking task. Furthermore, age of onset of epileptic seizures, number of seizures over lifetime as well as duration of seizures are known to be affect working memory and executive functioning (Black et al., 2010).

1.5.2. Afterdischarges and LTP

Previous research has examined the relationship between AD and LTP. It has been found that during the early development of kindling, an AD can lead to synaptic potentiation, which is referred to as postictal potentiation (PIP). However, there has been much debate regarding whether PIP is akin to LTP. Studies have shown that a non-competitive NMDA antagonist was only able to suppress LTP, having no effect on PIP (Leung & Shen, 1993; Gilbert & Mack, 1990; Cain et al, 1992), which implies that LTP and PIP may have a different mechanism that leads to their expression.

In a study conducted by Leung & Shen (1993), it was shown that duration of an AD was an important factor in determining potentiation magnitude; high-frequency stimulations that resulted in a short AD resulted in LTP comparable to that after a prime-burst stimulation paradigm (no AD), but high-frequency stimulations that evoked a long AD resulted in suppression of LTP. In an in-vitro study conducted by Moore and colleagues (1993), tetanic stimulation that evoked in an AD (13-33 s duration) in hippocampal CA1 slices was followed by depressed LTP as compared to control slices that did not induce an AD.

The effect of repeated seizures on LTP has also been an area of interest for researchers. Anwyl et al., (1987) showed that repeated electroconvulsive treatment led to marked inhibition of LTP in rat hippocampal slices. Leung & Wu (2003) also examined the effects of repeated seizures by employing the kindling paradigm and found that rats had suppression of LTP in the kindled paradigm as compared to controls. Similarly, a rodent model of hypoxia-induced neonatal seizures showed attenuation of LTP in the hippocampal CA1 region (Zhou et al., 2011). Another study concerned with the effects of a single neonatal seizure found that inducing the seizure in a rodent led to a decrease in the membrane pool of glutamate receptors and NMDA receptors, resulting in impaired CA1 hippocampal LTP (Cornejo et al., 2007). While various bodies of work have

examined this LTP suppression effect, whether it is caused by saturation of synaptic responses or an impairment of LTP-associated molecular mechanisms remains to be seen (Suarez et al., 2012).

1.6 Extracellular Field Potentials

Electrophysiological studies of the hippocampus can be conducted *in vitro*, using slice preparations, or *in vivo*. While *in vitro* studies allow for greater control and retain intrinsic connections that can be monitored, they require extrinsic projections to be severed. *In vivo* preparations are advantageous in that the entire brain is kept intact and only local damage is done through the insertion of electrodes. Recording electrodes are inserted into the extracellular space to measure field potentials. However, field potentials are not localized to a small space because currents and potentials are distributed across a conductive medium; this effect is called volume conduction. As such, field potentials are indirect measures of electrical activity from a single neuron or multiple neurons.

Due to its laminar organization, the hippocampus is an ideal brain structure for examining extracellular current flow. Pyramidal cells are lined up in parallel and synchronous activation during an evoked potential will summate field potentials from individual neurons to generate a large signal.

Current flows in a closed loop in a pyramidal cell, generating areas of positivity and negativity, effectively creating a dipole field. The opening of AMPA ion channels at the dendrites allows cations, or positive charges, to flow into a pyramidal cell. This leads to an intracellular increase in positive charges and membrane potential, while the extracellular space is negative, thus forming a current sink (Leung, 2010). The current flows in a closed loop to maintain electrical neutrality and flows from positive to negative potential; thus, a current source is the local volume where current flows from the intracellular to extracellular medium (Leung, 2010). A current sink represents

current flowing into the cell during relative membrane depolarization, whereas a current source represents current flowing out of the cell during relative hyperpolarization. Excitation of the basal dendrites causes current to flow into the basal dendrites and the soma, then out of the soma, generating a sink at the basal dendrites and a source at the soma (Fig 1.2; Leung, 2010).

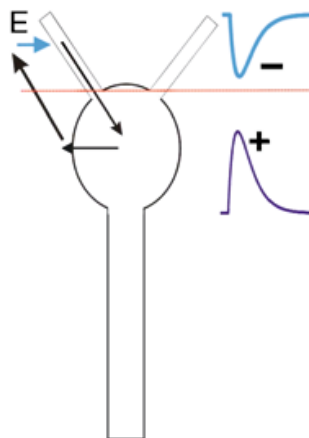


Fig 1.2. Evoked field potential during excitation of the basal dendrites, generating a current sink at the basal dendrites and a source at the soma (originally depicted by Leung, 2010).

Rationale and Hypothesis:

Previous research has attempted to characterize the interaction between AD and LTP by examining the effects of ADs on memory and learning processes associated with LTP as well as by determining shared characteristics between these two neural processes; however, there have been few studies examining the direct relationship between ADs and LTP in vivo. This study will attempt to fill this gap in the literature by examining how LTP responses in the mouse are affected by induction of ADs. We predict that an AD can lead to suppression of LTP magnitude for a duration greater than one hour, but less than one day.

Aims:

Aim 1: To determine if an AD can lead to suppression of LTP in the CA1

There have been studies that have shown that while LTP enhances memory and learning processes, AD affects memory task performance (Halgren & Wilson, 1985; Cain et al., 1993). This seems to indicate that AD affects similar pathways to LTP; however, the link between these two neural activities has not been explored. Therefore, we sought to study the effects that an AD can have on LTP magnitude.

Aim 2: To determine if LTP suppression is persistent over time

There is evidence that short-term deficits in memory lasted shortly after an AD (Halgren & Wilson, 1985; Cain et al., 1993). However, it is unclear whether the evocation of the AD might still have long-lasting effects that may not be behaviourally determined. Thus, we sought to study the effects of AD on LTP magnitude over the course of 1 day, as a means to determine if the AD still led to a dampening of LTP response magnitude.

Aim 3: To determine whether postictal depression of synaptic transmission and alteration paired-pulse facilitation are related to LTP suppression

Postictal depression following an AD has been a well-documented occurrence (Leung & Shen, 1993; Barr et al., 1997; Leung, 2017). One study conducted by Barr and colleagues (1997) found that LTP induction was inhibited during the initial phase of an AD in a rat hippocampal slice. However, it is unclear whether postictal depression and LTP suppression have the same mechanism.

Chapter 2: Methods

In order to observe the effects of an AD on LTP, two different experimental paradigms were conducted. Chronic experimental paradigms, with each mouse undergoing multiple sessions, were conducted in order to elicit long-term effects of an AD on LTP (i.e., for durations longer than 1 hour) and to observe any behavioural changes in the model organism due to AD stimulation. Acute experimental paradigms were conducted in order to identify factors of the AD that could lead to differences in effect on LTP.

Part I – Chronic Experiments

2.1 Animals for chronic recording

Seven adult male mice, weighing between 25 to 30 grams were used. Wild-type mice (3) and genetically modified mice that were deficient in the vesicular acetylcholine transporter (VACHT) were used. Mice with this deficiency had a targeted deletion of the VACHT gene; three mice had a complete deletion of this gene (knockouts or KO) while two knockdowns (KD) had only a heterozygous deletion of the gene. The purpose of having these additional groups of mice were to investigate whether there would be differences between the KO, KD, and WT both in their ability to generate LTP as well as how their responses would change once an AD was applied. Mice were housed in standard cage in a temperature-regulated environment and had ad libitum access to food and water. Experiments were conducted during the day (10 am – 5 pm).

2.2 Electrode Implantation

Mice were anesthetized using ketamine (100 mg/kg, i.p) and xylazine (25 mg/kg, i.p). Animal body temperature was maintained between 35° C and 36° C via a feedback-controlled heating pad connected to a rectal thermometer. The skull surface was exposed and oriented such that bregma and lambda were aligned on a horizontal plane. Paired electrodes were implanted bilaterally into the hippocampal CA1 region (P2.4, L 2.2). The ventral electrode of the pair was lowered to the

CA1 stratum radiatum, using electrophysiological criteria. The dorsal electrode of the pair, ~0.6 mm above the ventral electrode, was typically placed in the neocortex (layer 5). Single depth electrodes targeted the right stratum oriens (R3) and left stratum radiatum (L3) at AP -1.4, L \pm 1.5. Two screw electrodes were implanted over the frontal cortex and cerebellum, serving as the stimulus anode and recording ground, respectively. All depth electrodes were made of stainless steel wire, insulated with Teflon except at tips and approximately 0.005 inches in diameter. The exact electrode depth varied among animals and was adjusted based on electrophysiological response.

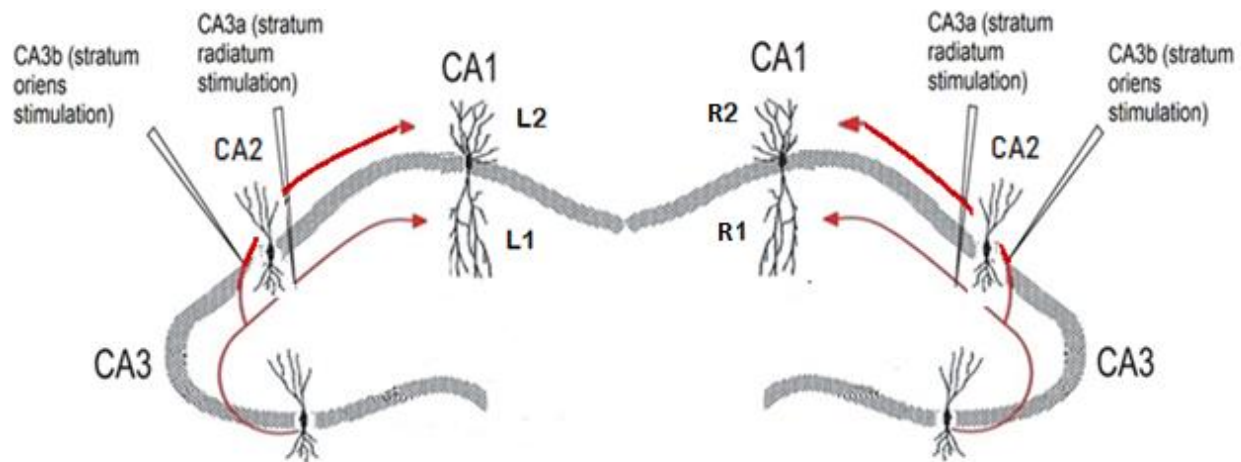


Fig 2.1 A coronal section of the mouse hippocampus, illustrating the position of stimulating and recording electrodes of hippocampal pathways. Electrodes were implanted into the CA1, the stratum radiatum, and the stratum oriens.

2.3 Experimental Procedure

Recording started at least one week after surgery, and after more than one habituation session, where the mouse was acclimated to the recording setup. The mouse was placed in its home cage and its electrodes were connected to a flexible cable. A stratum oriens electrode that evoked a basal dendritic field excitatory postsynaptic potential (fEPSP) in the CA1 was selected for stimulation.

Cathodal stimulus currents were delivered (with pulse duration of 0.2ms) through a photo-isolated stimulus isolation unit (PSIU6, Astro-Med/Grass Instrument). Stimulation repetition rate was <0.1 Hz. The stimulus threshold intensity was defined as the lowest stimulus intensity that evoked a detectable evoked potential (Leung & Shen, 1995). Potentials were amplified by a Medusa preamplifier followed by RA16 digital processors (Tucker Davis Technologies, Alachua, FL) and sampled at 24.4 kHz using custom-made programs (Fung et al., 2016). Average evoked potentials (AEPs; average of 4 sweeps) were acquired for all other electrodes at 2x threshold stimulus intensity. AEPs were recorded at ~5 min intervals, with stimuli delivered during behavioral immobility, when the mouse was not actively moving. When the baseline recordings were considered stable for >30 min, a tetanic stimulation was applied to induce LTP in different sessions in one mouse that were repeated at 1-2 weeks intervals, as described below.

2.3.1 Session 1: LTP induced by theta-frequency burst stimulation (TBS)

In the first session, after a 30-min baseline period, LTP was induced by 4 trains of theta-frequency burst stimulation (TBS), where 1 burst is defined as 1 pulse following 170 ms by 10 pulses at 100 Hz. TBS was delivered at 2x threshold stimulus intensity. Average evoked responses were recorded in 5 min intervals for 3 hours after TBS. Electrographic activity (EEG) was recorded during TBS to ensure that afterdischarges (ADs) did not occur. The rising slope of the resultant field excitatory postsynaptic potential (fEPSP) over a 1 ms duration was used to estimate the synaptic strength. The fEPSP slope at each electrode was normalized by the average slope during the 30-min baseline. LTP was defined as an increase in response by greater than one SE for three consecutive time points at >30 min after baseline.

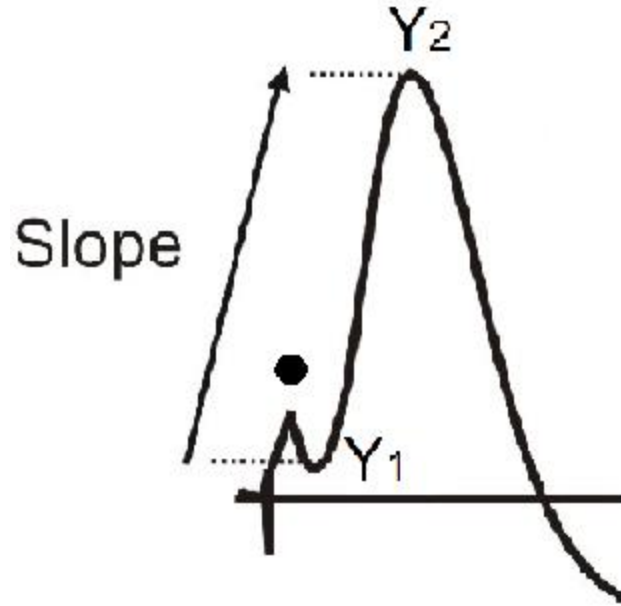


Fig 2.2. Slope measurements were taken from average evoked potentials. The slope of the field excitatory postsynaptic potential (fEPSP) was calculated at 1 ms for the duration of the rising phase. The filled circle indicates the stimulus artifact.

2.3.2 Session 2: AD followed 1h by TBS

In the next session, another stimulating electrode was selected to evoke an AD in the hippocampus (A-electrode); this electrode was different from the LTP-inducing electrode (L-electrode). An AD was operationally defined as high-amplitude paroxysmal discharges of at least two times the average baseline amplitude that followed the stimulation. Baseline single pulse L- and A-evoked responses were recorded for 30-min, before an AD was induced through the A-electrode with a high-frequency train of 200 Hz for 1s, at 4 x threshold stimulus (at $\geq 150 \mu\text{A}$). The AD was confirmed by electrographic recording of spontaneous EEG activity from selected electrodes of the 16-channel array, which included an electrode near the hippocampal fissure (typically 12th electrode of the array). Both single and average responses (stimulation of both A- and L-electrodes) were recorded on the computer. Recordings were made for 60 minutes after an AD, after which TBS was delivered to the L-electrode in an attempt to induce LTP. Average evoked potentials were then recorded for 3 h post-TBS.

2.3.3 Session 3: TBS alone

One week after the 1h paradigm, the TBS protocol was administered once more without administering an AD. After a 30-min baseline, TBS was delivered and recording was continued for 3h. This was referred to as the LTP sandwich experiment.

2.3.4 Session 4 and 5: AD followed 1 day by TBS

The next experiment, conducted one week TBS control, was an AD only paradigm. An AD was induced through the A-electrode with a high-frequency train of 200 Hz for 1s, at 4x the threshold stimulus (with a minimum of 150 μ A). The AD was confirmed by EEG recording, and evoked responses (from both A- and L-electrodes) were recorded for at least 3h after an AD. The following day, TBS was delivered to the L-electrode in an attempt to induce LTP; this was the 1 day paradigm.

Some mice underwent additional sessions to record LTP that was induced 1 week after this AD induction; this was referred to as the 1 week paradigm. Only mice that had maintained the same threshold for baseline and TBS were selected for the 1 week paradigm.

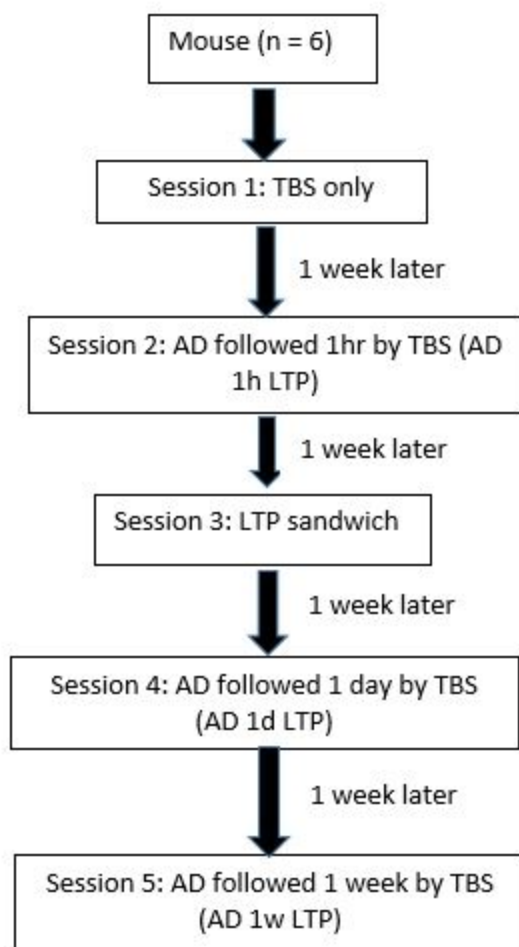


Fig 2.3 Flow chart representing timeline of experiments proposed for all mice (WT, KO, and KD) in the chronic experimental paradigm.

2.4 Perfusion

After completion of the experiments, mice were euthanized with 0.2 ml of pentobarbital (60 mg/ml). The mice were intracardially perfused with 50 ml of saline and 50 ml of 4% formaldehyde solution. The brain was then extracted from the cranium and stored in a 4% formaldehyde solution for 48 hours prior to sectioning.

2.5 Histology and Staining

Brains were frozen on a freezing microtome and sliced into 40 μm thick sections. Slices were then mounted onto slides and stained with thionin. Electrode locations were identified using light microscopy (Fig 2.4).

2.6 Statistical Analysis

For experiments assessing the effect of AD on LTP (i.e., 1-hour, 1-day, and 1-week paradigms), a three-time-point running average was applied to reduce variability. Two treatments were compared using the same subjects –initial LTP only, and LTP following induction of an AD. A two-way randomized block ANOVA (group x time) was used to compare the treatments to determine whether the main (group) effect or interaction (group x time) effect was significant at the $p < 0.05$ level. If a significant main or interaction effect was found, a post-hoc Fisher's LSD was conducted.

Stimulation of an electrode in stratum oriens, on the same or contralateral side, typically resulted in a basal dendritic response. The basal dendritic response in the dorsal hippocampus was characterized as being negative above the CA1 cell layer, and positive below (Fig 1.2). The potential polarity reflects excitatory currents entering the basal dendrites (stratum oriens) and leaving the cell bodies and apical dendrites (Leung, 2010).

Evoked potentials were acquired by selective stimulation during behavioral immobility, when the mouse was standing or sitting still without gross movements. Previous studies indicated that active movements may greatly reduce the apical dendritic fEPSPs, but only marginally reduced the basal dendritic fEPSPs (Leung, 1980). However, responses at 2 x the threshold stimulus intensity (40 to 100 μA) during the baseline still showed considerable variation, possibly attributed to movement artifacts and lack of behavioral clamping.

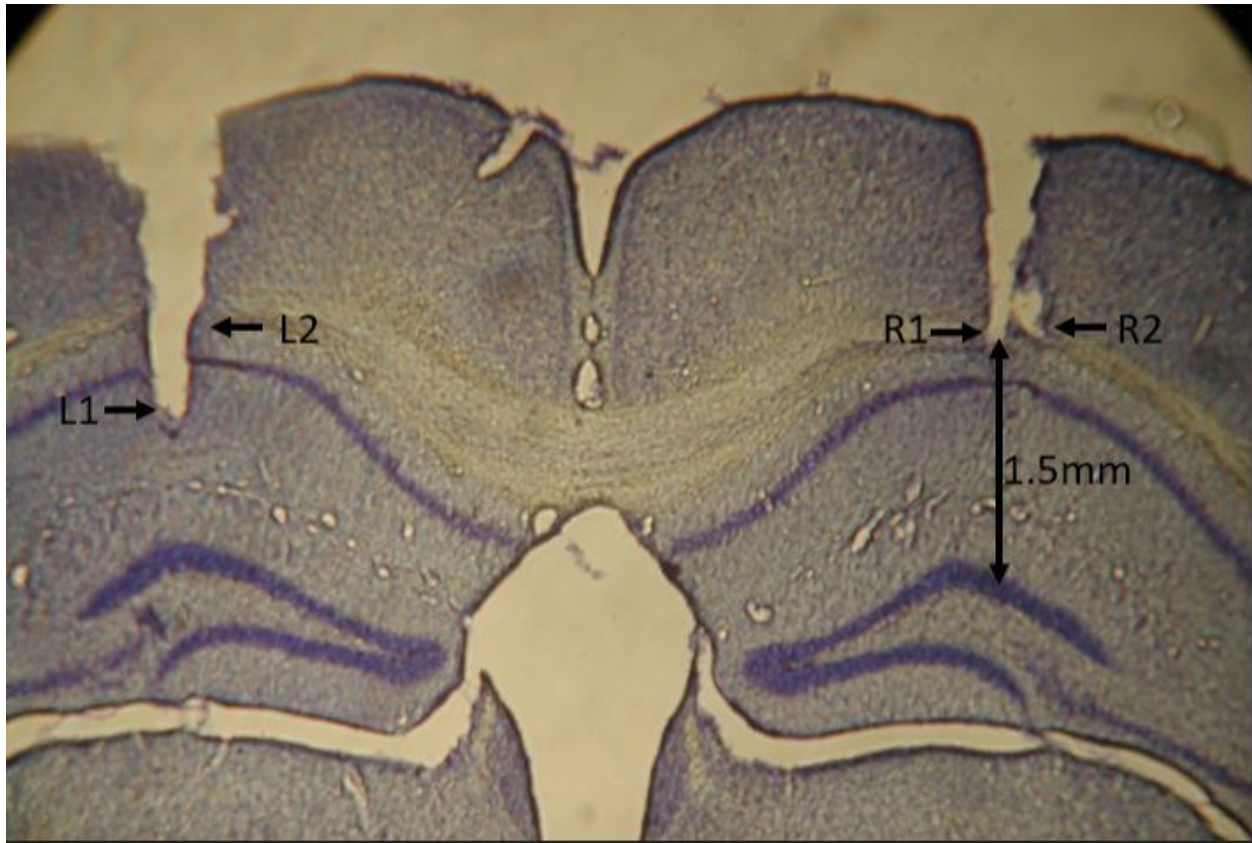


Figure 2.4. A coronal section of the hippocampus in a representative mouse (VRM07), illustrating the position of stimulating and recording electrodes. L1 and L2 indicate paired electrodes implanted bilaterally into the hippocampal CA1 region, as do R1 and R2; L1 and R1 are the ventral electrodes of the pair, lowered to the CA1 stratum radiatum (P2.4, L2.2). L2 and R2 are the dorsal electrodes of the pair, placed in the neocortex layer 5 (P2.4, L 1.6).

Part II – Acute Experiments

2.7 Animals for acute recording

Twelve adult, male mice, weighing between 20 and 50 grams were used. Wild-type mice and genetically modified mice deficient in the ATRX gene (ATRX loxP Cre-recombinase model) were used. Previous research has shown that deletion or mutation of the ATRX gene results in ATRX syndrome, which is an intellectual disability disorder linked to learning deficits in behaviour including an inability to generate LTP (Nogami et al., 2011). The purpose of having these additional groups of mice were to investigate whether there would be differences between the ATRX-modified and WT both in their ability to generate LTP as well as how their responses would change once an AD was applied. The ATRX-modified mice for this study had deletion of ATRX only in the forebrain-specific pyramidal neurons (Tamming et al., unpublished).

2.8 Electrode Implantation

Stimulating electrodes were constructed out of stainless steel wires, 0.005 inch in diameter, insulated with Teflon except at the tips. Silicon recording probes were purchased from NeuroNexus, Ann Arbor, MI. Silicon recording probes had 16 recording sites spaced 100 μm apart on a vertical shank.

2.9 Surgery

Mice were anesthetized using 10% urethane anaesthesia (1 g/kg solution, i.p.) and placed in a stereotaxic surgery apparatus. Atropine methyl nitrate was administered (5 mg/kg, i.p.) to reduce airway secretions throughout the system. Animal body temperature was maintained between 35 and 37 degrees Celsius via feedback-controlled heating pad connected to a rectal thermometer. The skull surface was exposed and oriented such that bregma and lambda were in a horizontal plane. Stimulating electrodes were lowered into the left (iCA3) and right (cCA3) CA3 regions to stimulate Schaeffer collaterals projecting from hippocampal area CA3 to CA1. The 16-channel

silicon probe was lowered into area CA1 of the left hippocampus to record evoked field excitatory postsynaptic potentials (fEPSPs). The exact electrode depth varied among animals and was adjusted based on electrophysiological response. Two screw electrodes were implanted over the frontal cortex and cerebellum, serving as the stimulus anode and recording ground, respectively.

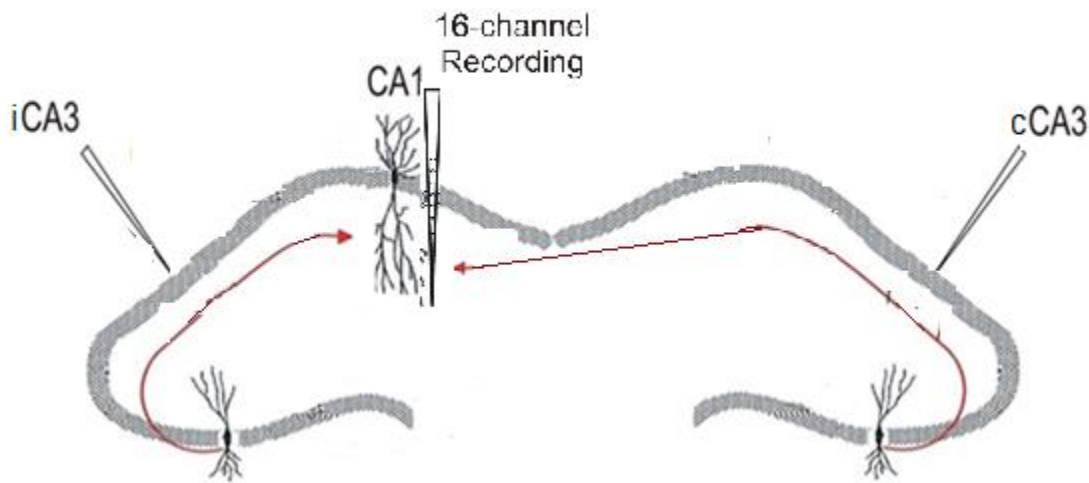


Fig. 2.5. A coronal section of the mouse hippocampus, illustrating the position of stimulating and recording electrodes of hippocampal pathways. Electrodes were implanted into the CA1, the ipsilateral CA3 (iCA3), and the contralateral CA3 (cCA3).

2.10 Acute experimental procedure

Signals from the 16-channel recording probe were amplified 10x by a TDT (Tucker-Davis Technology) headstage, a 16-channel Medusa preamplifier and fed by optic fibres to TDT digital processors (RA16 Base Station). Signals were digitized at 6.1- 24.4 kHz by TDT real-time processors and custom-made software from our lab. Stimulus pulses (0.2 ms duration) were delivered through a photo-isolated stimulation unit (PSIU6, AstroMed/Grass Instrument).

Baseline evoked responses were monitored at 2x threshold intensity at a sampling rate of 24.4 kHz for 4096 samples. Four sweeps were taken at 0.1 Hz and averaged to generate an averaged evoked

potential at a particular time. Synaptic and action currents spread due to volume conduction; therefore, a technique known as current-source density (CSD) analysis was used to remove the effects of volume conduction and identify the macroscopic locations of current sources and sinks. A one-dimensional CSD was calculated from the field potential. CSD (z, t) as a function of depth z and time t was calculated by a second-order differencing formula:

$$\text{CSD}(z, t) = \sigma [2 \Phi(z, t) - \Phi(z + n\Delta z, t) - \Phi(z - n\Delta z, t)] / (n\Delta z)^2 \text{ (Equation 1)}$$

where $\Phi(z, t)$ was the potential at depth z and time t , Δz was the spacing (100 μm) between adjacent electrodes on the 16-channel probe. The conductivity σ was assumed to be constant and the CSDs were reported in units of V/mm^2 . CSD analysis in this study used an effective step size of 200 μm , i.e., $n=2$ in equation 1, which was equivalent to CSD obtained following 1-2-1 spatial smoothing (Freeman and Nicholson, 1975; Leung, 2010). The maximal slope (of 1 ms duration) during the rise of the maximum excitatory sink was used to assess the magnitude of the excitatory response.

After a 30 min baseline period, an AD was induced at the iCA3 electrode with a high-frequency train of 100 Hz for 5 s at a stimulus intensity of 500 μA and 0.2 ms pulse duration. AD was confirmed by polygraph EEG recording, and it is operationally defined as high-amplitude paroxysmal discharges of at least two times the average baseline amplitude. Responses evoked by stimulation of either iCA3 or cCA3 electrode were recorded at 5 min intervals for at least 1h after the AD. At 63 min post-AD, LTP was induced by 4 trains of theta-frequency burst stimulation (TBS), where 1 train consisted of 10 bursts at interburst interval of 200 ms, and each burst contained 10 pulses at 100 Hz. TBS was delivered at 2x threshold stimulus intensity. Average evoked responses were recorded every 5 min for 2 hours after TBS. The maximal slope (of 1 ms duration) during the rise of the maximum excitatory sink at the basal dendritic (stratum oriens) was used for LTP assessment (Fig 2.6).

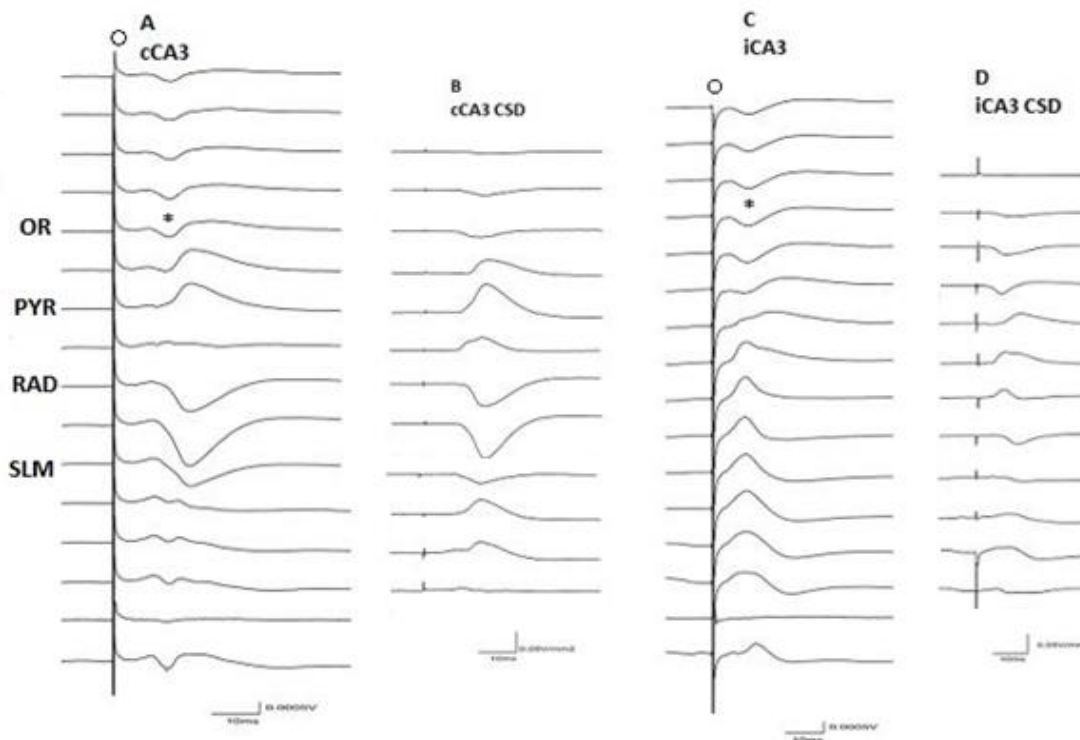


Fig. 2.6. Average evoked potentials (AEPs: A and C) and current source density (CSD: B and D) transients in CA1 from representative mice following contralateral CA3 (A and B) or ipsilateral CA3 (C and D) stimulation. Potentials were recorded by a 16-channel electrode silicon probe with 100 μm interval between electrodes. (A) AEPs (average of 4 sweeps) following stimulation of the contralateral CA3 at 50 μA (2x threshold). (B) CSD profile derived from the AEPs shown in (A). Stimulation generated a current sink in the CA1 basal dendrites. (C) AEPs (average of 4 sweeps) following stimulation of the ipsilateral CA3 at 60 μA (2x threshold). (D) CSD profile generated from the AEPs shown in (C). Stimulation led to a current sink at the basal dendrites, indicated with an asterisk. Open circle indicates shock artifact. Legend: OR, stratum oriens; PYR, stratum pyramidale; RAD, stratum radiatum; SLM, stratum lacunosum moleculare.



Fig 2.7. Flowchart representing timeline of experiment for all mice in the urethane-anesthetized acute paradigm.

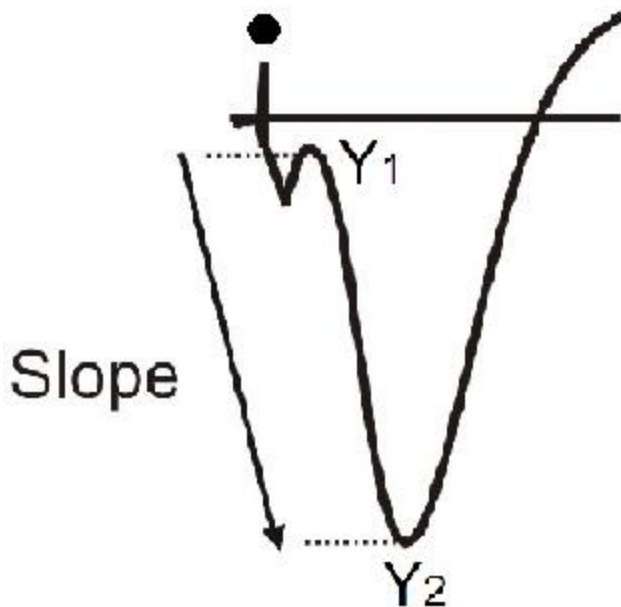


Fig. 2.8. Slope measurements were taken from CSD traces. The slope of the excitatory sink was calculated at 1 ms for the duration of the rising phase of the excitatory sink (Y1 to Y2), and the value of the maximal magnitude of the slope was taken as the estimate of the slope. The filled circle indicates the stimulus artifact.

2.11 Perfusion

After completion of the experiments, mice were euthanized with 0.2 ml of pentobarbital (60 mg/ml). The mice were intracardially perfused with 50 ml of saline and 50 ml of 4% formaldehyde solution. The brain was then extracted from the cranium and stored in a 4% formaldehyde solution for a minimum of 48 hours prior to sectioning.

2.12 Histology and Staining

Brains were frozen on a freezing microtome and sliced into 40 μm thick sections. Slices were then mounted onto slides and stained with thionin. Electrode locations were identified using light microscopy.

2.13 Statistical Analysis

When CSD responses were plotted over time, there was considerable variation in response at a single time point, thus running averages of three consecutive time points were used.

Three different relationships were examined: the relation between postictal depression (responses after an AD) and the AD duration, the relation between LTP (responses after TBS) and AD duration, and the relation between LTP response and postictal depression. Microsoft Excel was used for graphing and trendline analysis. Regression analysis was also conducted for each of the aforementioned relationship, with linear and/or polynomial models used (if linear appeared to be non-significant).

Chapter 3: Results

3.1 LTP induced by theta-frequency burst stimulation (TBS)

A TBS protocol of 4 sweeps each with 4 trains of theta-frequency bursts was applied to induce LTP in the CA1 region in vivo. The intensity used for tetanic stimulation ranged from 40 to 200 μ A, which was 2 to 4 times the threshold, and was always below that required to induce an afterdischarge (AD). TBS led to an enhancement of the basal dendritic response slope; this was consistent across all experiments and experimental groups. A representative experiment illustrates LTP of the basal dendritic response in CA1 (Fig 3.2A). The size of the basal dendritic response slope of the evoked potential increased as compared to the baseline (Fig 3.1).

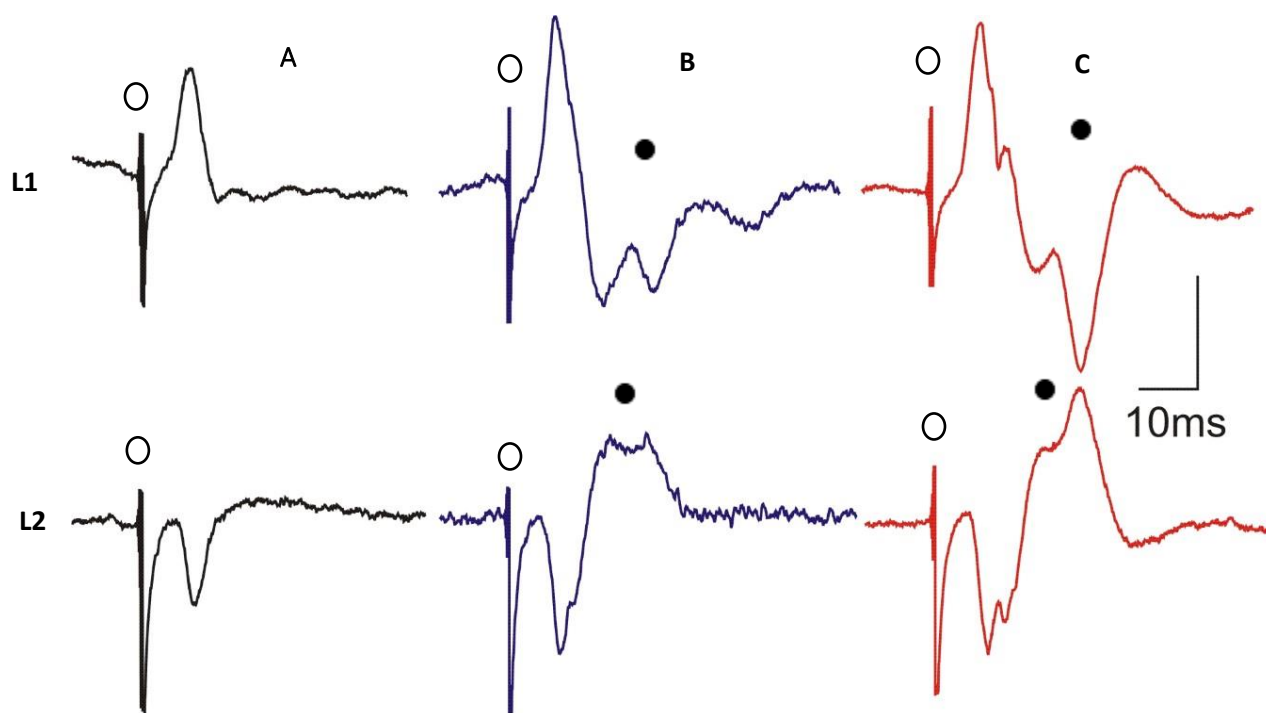


Fig. 3.1 AEPs evoked by stimulation of the contralateral hippocampus in a representative mouse (VRM07, see Fig. 2.3) during an experiment intended to induce LTP by a theta-burst stimulation (TBS). *A*: Baseline response at <30 min before TBS. *B*: Response at 5 min post-TBS. *C*: Response at 1 h post-TBS. An early basal dendritic response was characterized by a negative response at L2 (stratum oriens) and positive response at L1 (stratum radiatum), see Fig. 2.3 for histological section. Late response (indicated by filled circle) indicated multisynaptic activation through the CA3-CA1-EC-hippocampus loop (Wu & Leung, 2003). Open circle indicates shock artifact.

When plotted over time, there was considerable variation in the response at a single time point, thus running averages of three consecutive time points were used (Fig 3.2B). The magnitude of the basal dendritic LTP was initially large, but decayed after the first hour post-TBS (Fig. 3.2). The slope of the response soon returned to baseline levels and then stabilized for the remainder of the experiment. This was seen in all mice and is characteristic of TBS-induced basal dendritic LTP.

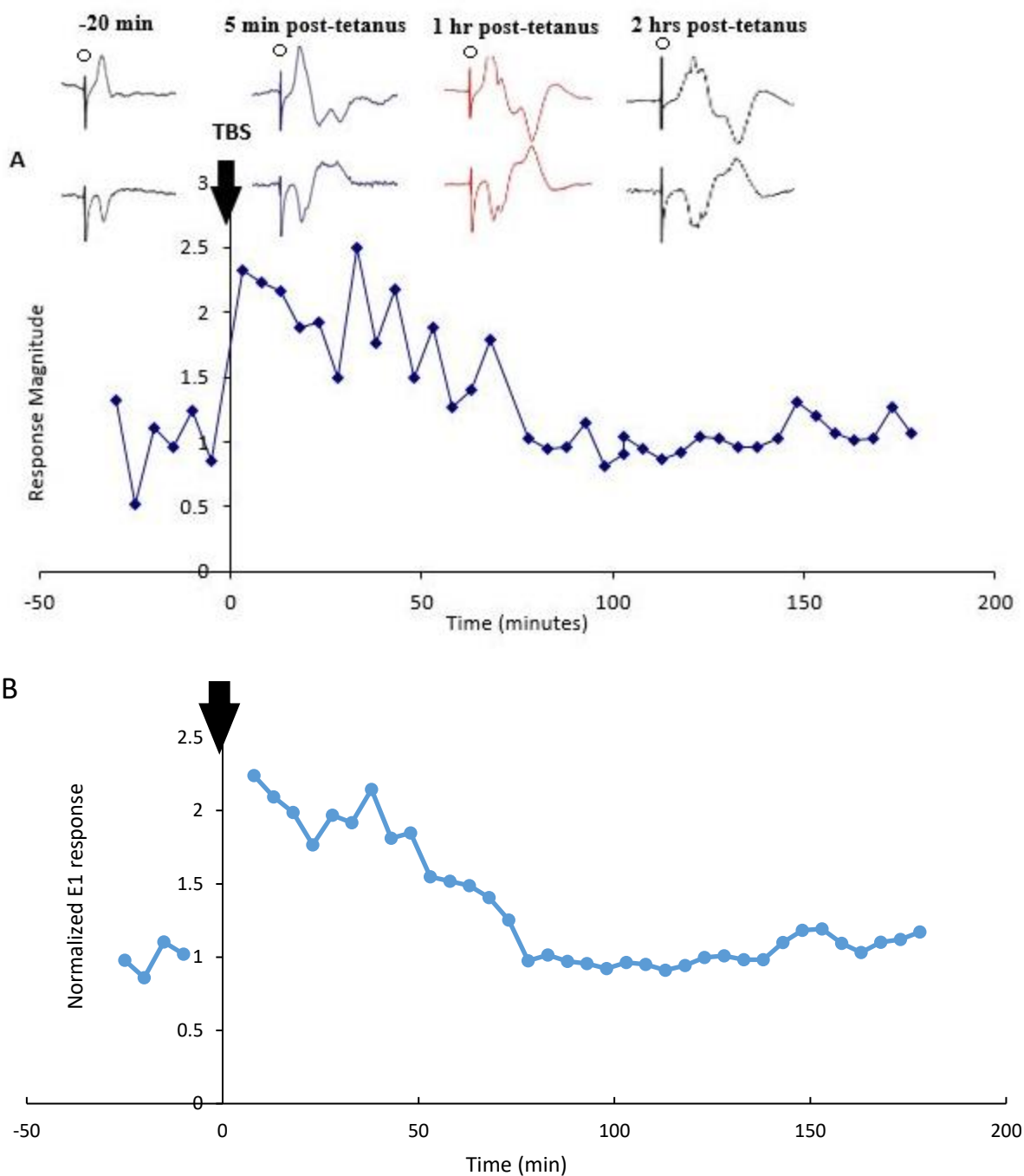


Fig 3.2. Data from a representative experiment (VRM07) where TBS was applied to the R1 electrode at time zero (black arrow) with AEPs recorded at the L1 electrode. (A) The slope response (E1) of the AEPs at L1 was analyzed during a 30-min baseline followed by 3 h of post-TBS. Top traces show AEPs at L1 and L2 electrodes, at different times; stimulus artifacts indicated by open circle. TBS of 80 μ A intensity was applied at time zero (black arrow) after 30-min baseline. (B) Running average of 3 consecutive time points of the slope response.

3.2 AD followed 1h by TBS

A high-frequency train of 200 Hz for 1 s was applied to induce AD in the CA1 region. The stimulus intensity used to evoke an AD ranged from 160 to 400 μ A, which was usually 4 times the threshold intensity to induce a single-pulse response.

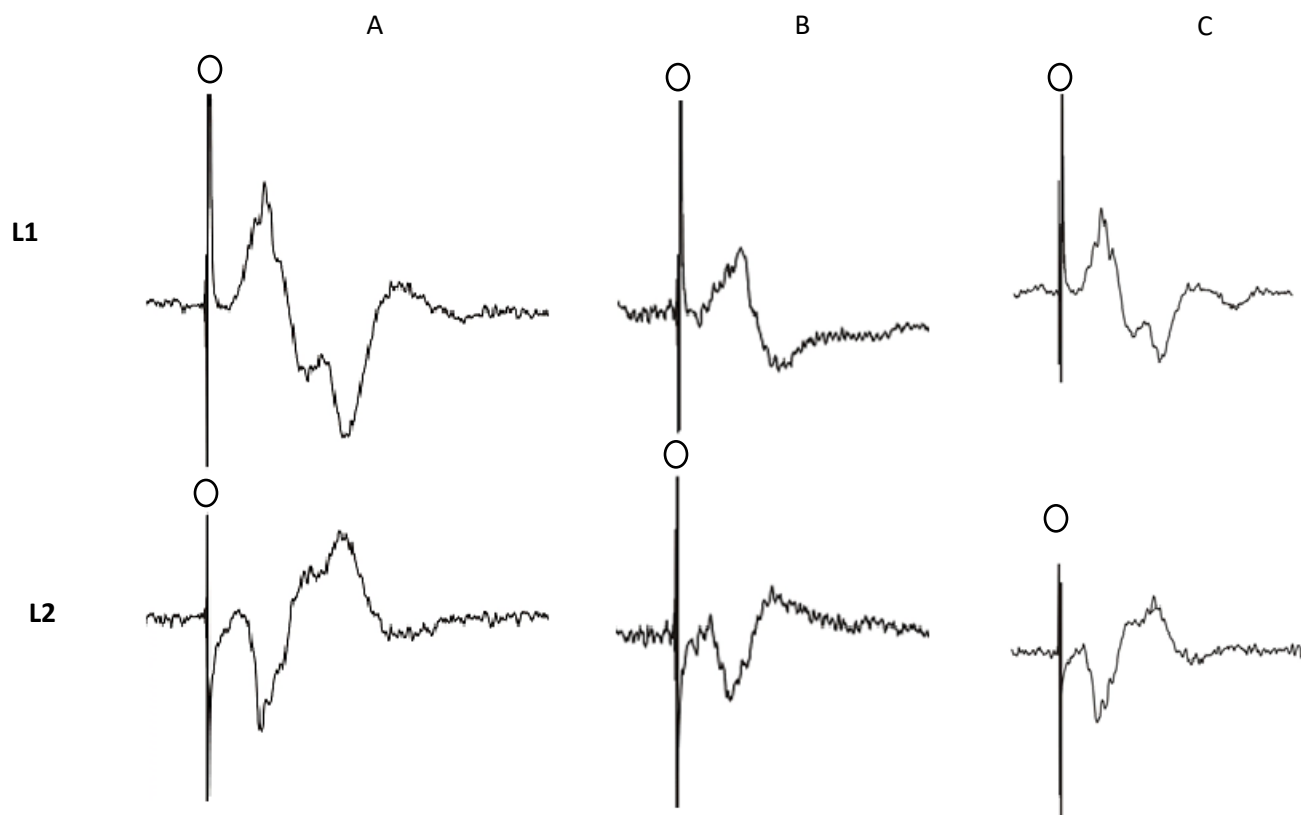


Fig. 3.3 AEPs of basal dendritic response of a representative mouse (VRM07) during the AD-1h LTP experiment. *A*: Baseline response at < 30 min before high-frequency stimulation that evoked an AD of 28 s. *B*: Response at 5 min post-AD, showing strong postictal depression. *C*: Response at ~1 h post AD shows a smaller postictal depression than that at 5 min. Open circle indicates shock artifact.

A representative experiment illustrates basal dendritic response in CA1 before and after AD stimulation (Fig. 3.3, Fig. 3.4). Behaviourally, during the first few seconds of the 28-s AD evoked, the mouse was immobile, looking alert with eyes wide open. After the AD ended, the mouse would

move around vigorously before settling back into its normal pace of movement. The AD resulted in suppression of the basal dendritic fEPSP at both L1 and L2 electrodes in CA1 (Fig. 3.3). The postictal suppression was large in the first 30 min after an AD, but dissipated at ~ 1 h. TBS was applied at 1 h post-AD, and it did not induce behavioural changes. Following TBS, the responses were potentiated immediately, and the magnitude of potentiation declined in the next 3 h (Fig 3.4A). When plotted over time, there was considerable variation in response at a single time point, thus running average of three consecutive time points were used (Fig 3.4B).

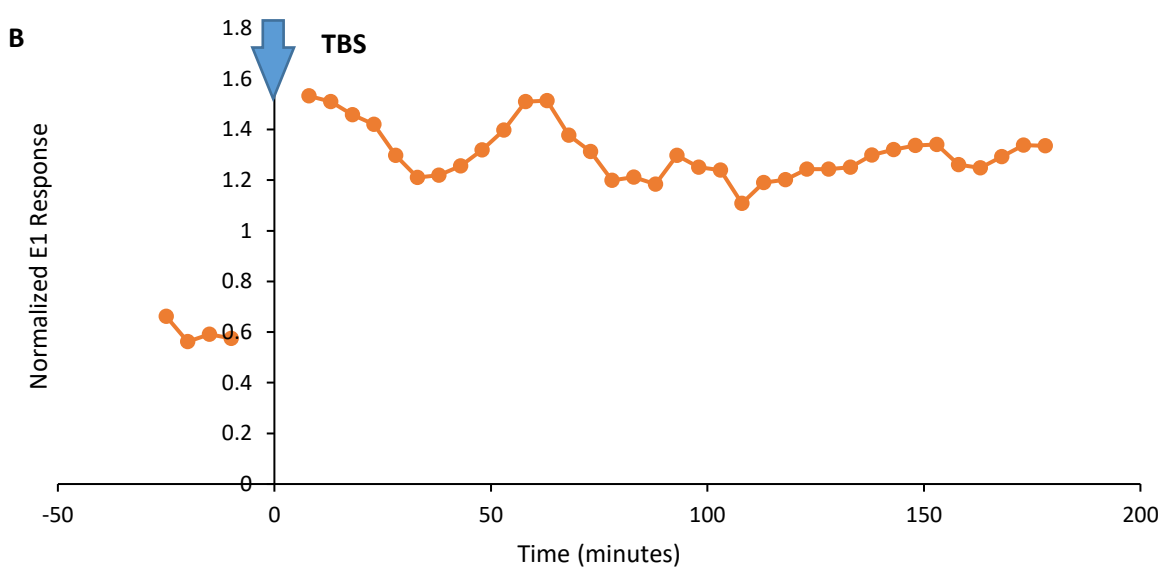
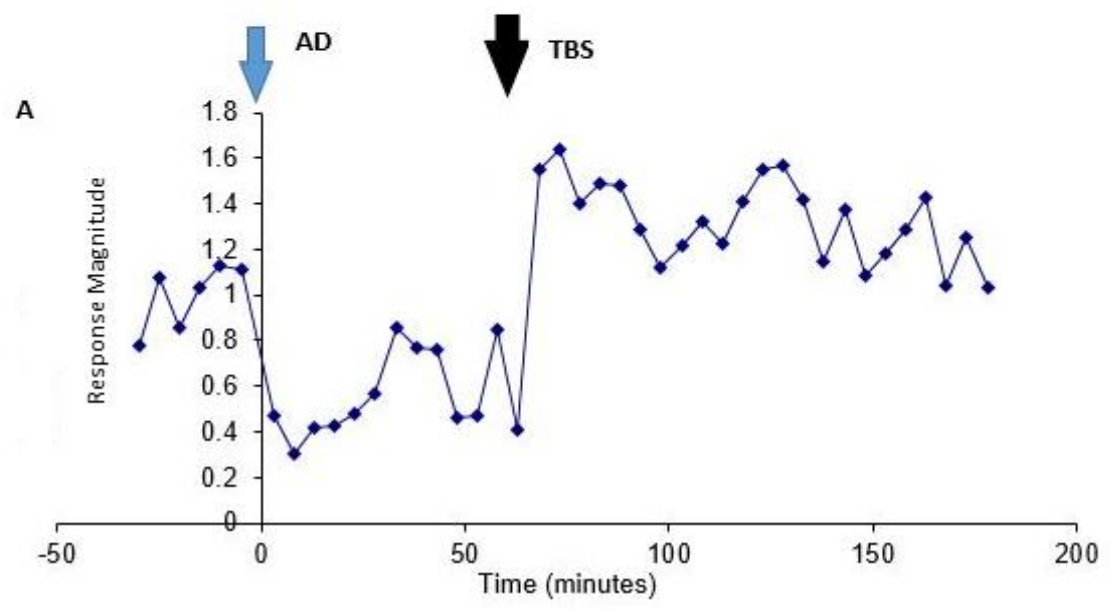
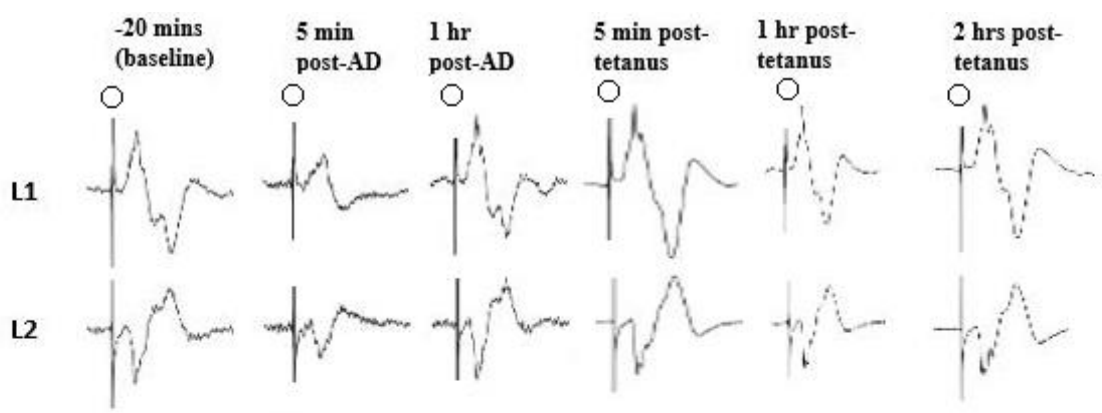


Fig. 3.4 Data from a representative experiment where an AD was applied at time zero (blue arrow), after a 30-min baseline, followed by TBS (LTP induction; black arrow) applied to the R1 electrode at time 60 min with recording from the L1 electrode. (A) Slope response of the AEPs from CA1 (electrode L2) during an experiment in a representative mouse (VRM07). Response was normalized by the average response slope during baseline. AD was applied to R2 electrode (see figure 2.6 for electrode placement) at 240 μ A at time 0, evoking an AD of 28s in CA1; TBS was applied at 80 μ A at 63 min post-AD. Top traces show AEPs at L1 and L2 electrodes, at different times (B) Running average of the normalized slope response for 30 min before, and 180 min after TBS, where three consecutive time points were averaged.

In the third session, repeating the TBS alone without AD also induced robust LTP, which was higher than that of the first TBS-alone session in this mouse (Fig. 5). In the fourth session, one day after an AD was induced in CA1, TBS induced a robust LTP, similar to the previous TBS-alone LTP (Fig. 3.5).

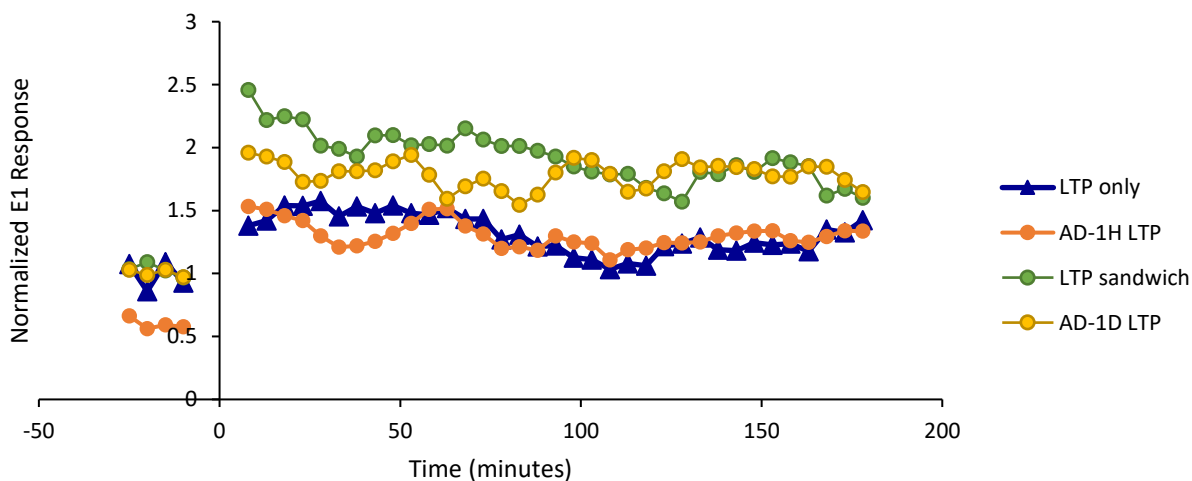


Fig. 3.5 Data from a representative mouse (VRM07) displaying LTP response curves according to the various paradigms: LTP-only, AD-1h LTP, LTP sandwich and AD-1D LTP. Responses are running averages of the slope response for 30 min before, and 180 min after TBS, where three consecutive time points were averaged. Response was normalized by the average baseline response before AD stimulation.

3.2.1 AD-1h LTP vs. LTP only, all mice

LTP and AD-1h LTP experiments were also performed on vAChT knockout (KO) and knockdown (KD) mice. There was no significant difference in the LTP between 3 WT, 2 KO mice, and 1 KD mouse, and their response to AD; thus, the data were grouped together for the 5 mice. In LTP only experiments of the combined group, TBS induced immediate potentiation of 200%, which decreased over 3 h. Paired AD 1h-LTP experiments showed weaker potentiation after TBS. A randomized-block, two-factor ANOVA revealed a non-significant effect of treatment ($F_{1,340} = 3.60$, $p_{\text{treatment}} = 0.1161$), but a significant treatment x time interaction effect ($F_{33,340} = 1.75$, $p_{\text{interaction}} = 0.0126$). Further examination using a post-hoc Newman-Keul's test revealed the largest deviation between groups to be < 30 min after LTP induction.

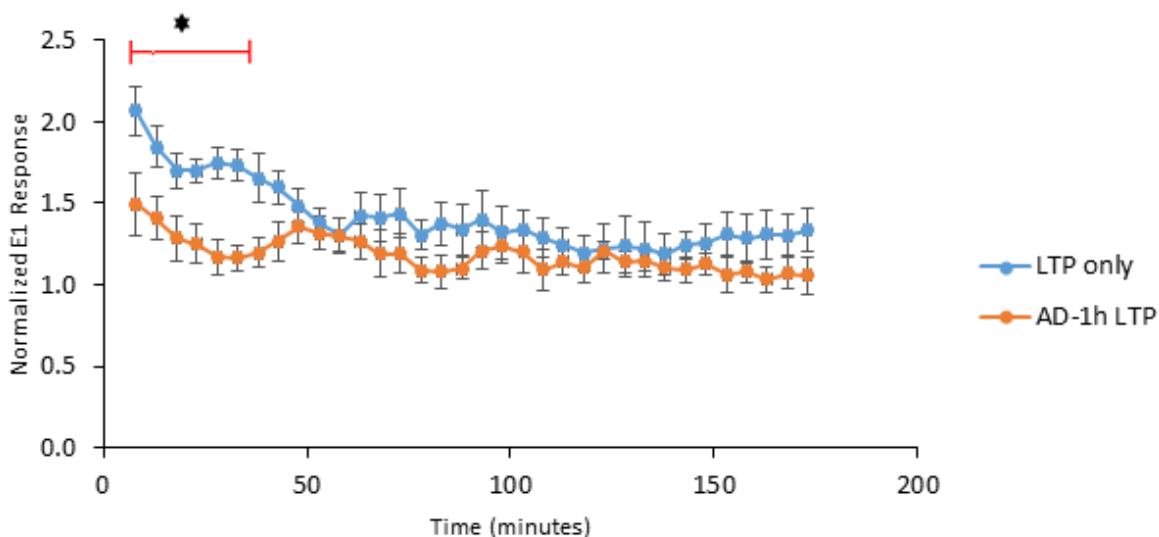


Fig.3.6 Normalized E1 post-TBS response curves for the LTP-only and AD-1h LTP treatments, including all mice (wildtype and VACHT knockout and knockdown n=6). Baseline response was set at 1 for 30 mins prior to TBS stimulation (excluded from graph). TBS was delivered at time 0.

3.2.2 AD-1d LTP vs. LTP only, all mice

In 4 mice, TBS was given 1 d after an AD, and compared to the LTP only data (Fig. 3.7). For both treatments, TBS induced immediate potentiation of 200% that decreased over 3 h. A randomized-block, two-factor ANOVA of the post-TBS responses at 1d post-AD and for LTP-only did not reveal a significant treatment effect ($F_{1, 210} = 0.044$, $p_{\text{treatment}} = 0.8408$) or a treatment x time interaction effect ($F_{34, 210} = 0.44$, $p_{\text{interaction}} = 0.9972$). Some mice underwent the 1 week post-AD paradigm (Fig. 3.8; 2 WT, 1 KO, and 1 KD, $n=4$); mice were selected for this session if thresholds remained consistent as compared to previous experiments. A randomized block, two-factor ANOVA of the post-TBS responses at 1 week post-AD and for LTP-only did not reveal a significant treatment effect ($F_{1,204} = 1.10$, $p_{\text{treatment}} = 0.332$) or a treatment x time interaction effect ($F_{33,204} = 0.506$, $p_{\text{interaction}} = 0.998$).

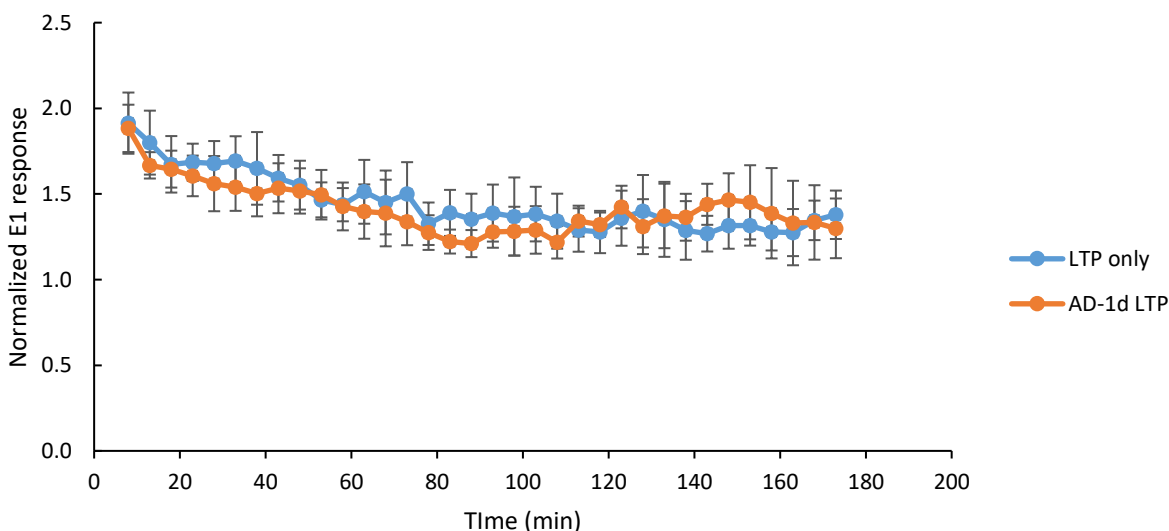


Fig.3.7 Post-TBS response curves for the 1d post-AD experiments, averaged across 4 mice (2 wildtype, 1 VACHT knockout and 1 VACHT heterozygous mice). TBS was delivered at time 0. The LTP only group were from experiments done in the same 4 mice.

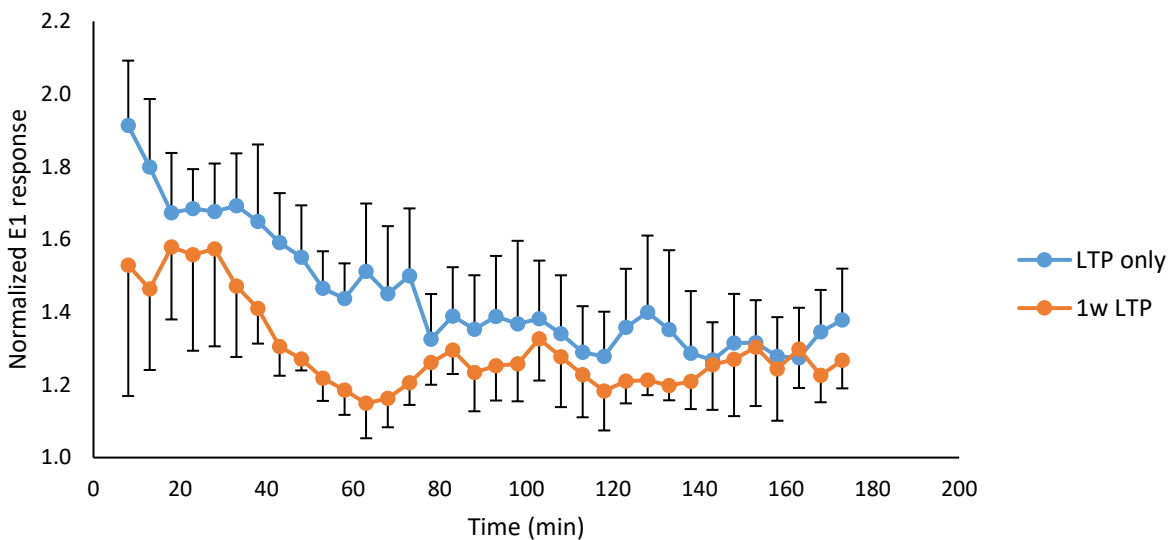


Fig 3.8 Post-TBS response curves for the 1w post-AD experiments, averaged across 4 mice (2 wildtype, 1 VACHT knockout and 1 VACHT heterozygous mice). TBS was delivered at time 0. The LTP only group were from experiments done in the same 4 mice.

3.2.3 Postictal depression vs AD duration in behaving mice

The postictal phase was recorded for first 60 min following AD. Fig.3.9 shows the average depressed response values following delivery of an AD in a group of 6 mice (1 AD per mouse). The relation between postictal response and AD duration shows a strong inverse quadratic relationship at early times (8 min) post-AD; Fig.3.10). However, this relation appears to weaken over time (Fig. 3.10). The quadratic relation suggests that depression could be strong with either short (< 2 s duration) or long ADs, however there was only one data point for short AD, which was for the VACHT KO mouse.

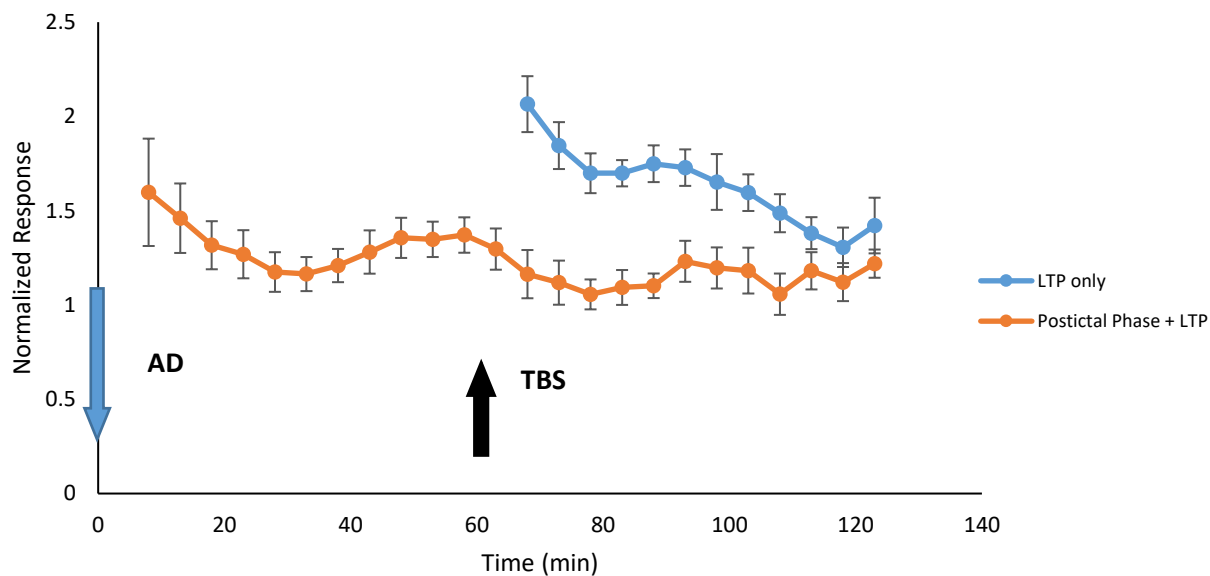
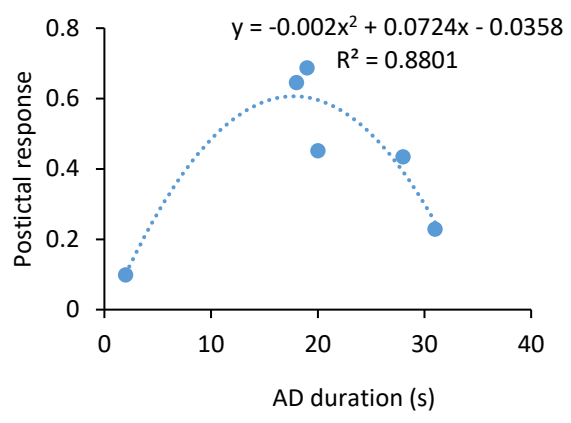
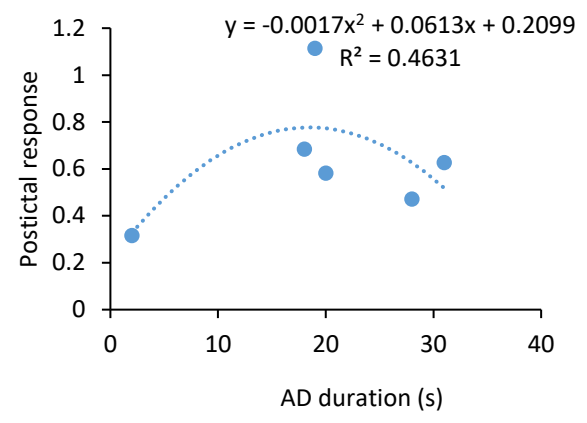


Fig.3.9. Mean basal dendritic fEPSP slope values for the group (n=6) for both the LTP only and the AD-1h LTP treatments. The AD treatment values include the postictal phase for the AD treatment, and TBS was delivered at 60 min. LTP-only experiments had no prior AD, but were shifted to indicate the same time of TBS as in the AD-1h group. All error bars depict the standard error of the mean.

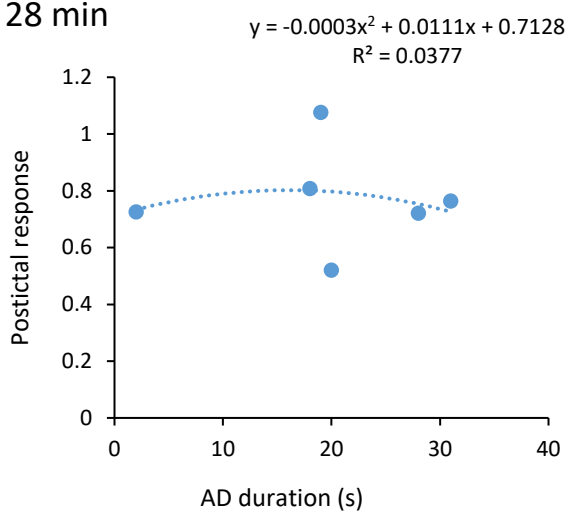
8 min



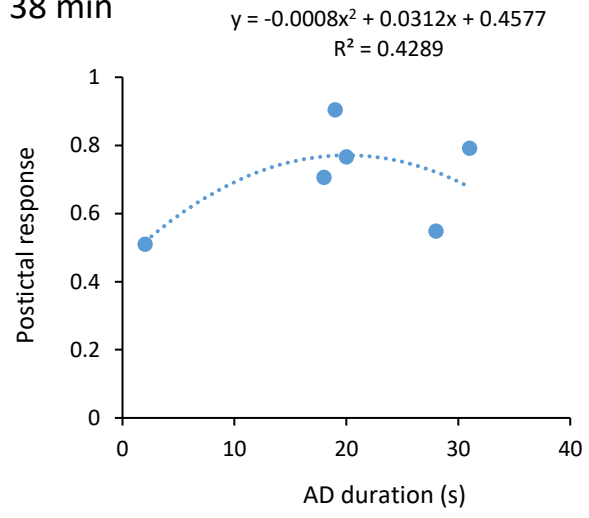
18 min



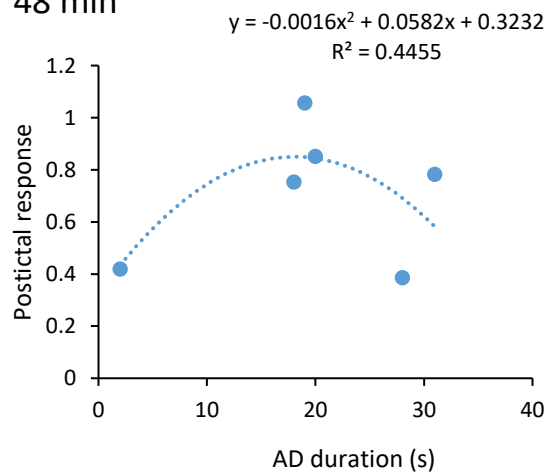
28 min



38 min



48 min



58 min

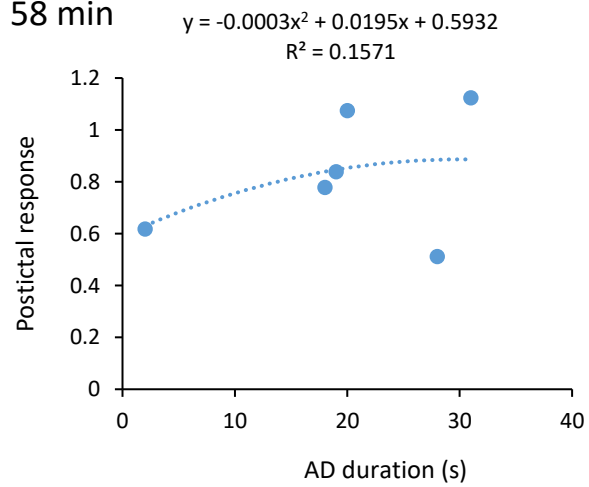


Fig.3.10 A series of graphs depicting the relation between postictal response (y) (normalized by average baseline response) to AD duration (x) at different times after the AD for a group of 6 mice. Each point indicates result from one animal. Postictal response at times 8, 18, 28,38, 48, 58 min after the AD Quadratic models were used to depict the relationship between the variables; linear models show lower R^2 values.

3.2.4 LTP vs AD duration in behavioural mice

Previous results (See Section 3.2.1) suggested that the effects of an AD on LTP were most prominent at times < 30 min post-TBS. The relation between AD-1h LTP and AD duration was examined by plotting LTP versus AD duration, which varied between 2 – 31 s in different mice. A plot of the 18 min post-TBS response (LTP response) with AD duration showed a positive linear correlation ($R^2 = 0.374$; Fig. 3.11), although the positive slope was not statistically different from zero ($F_{1,4} = 2.39$, $p = 0.197$).

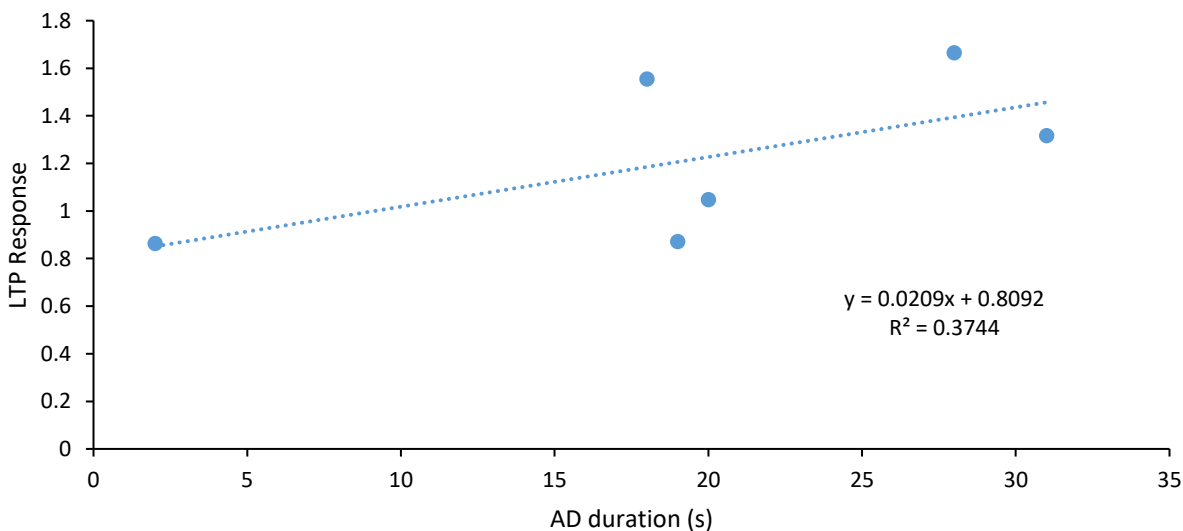


Fig.3.11. A graphical presentation of the linear model proposed to represent the relationship between mean LTP response at 18 min post-TBS (y) and AD duration (x), with durations ranging from 2s – 31s. The dotted trace was the best line fit with linear regression analysis, showing the equation for the line and goodness of fit R^2 . Each point indicates results from one animal.

3.2.5 Postictal depression vs LTP

Response data during postictal depression for the first 60 min following AD was compared to LTP response data (18 min post-TBS). The correlation between postictal depression and post-TBS response data appeared to be very weak (Fig. 3.12; $R^2 = 0.0568$). Linear regression analysis showed that the linear relation between post-TBS response and postictal response was not statistically significant ($F_{1,4} = 0.24$, $p = 0.649$).

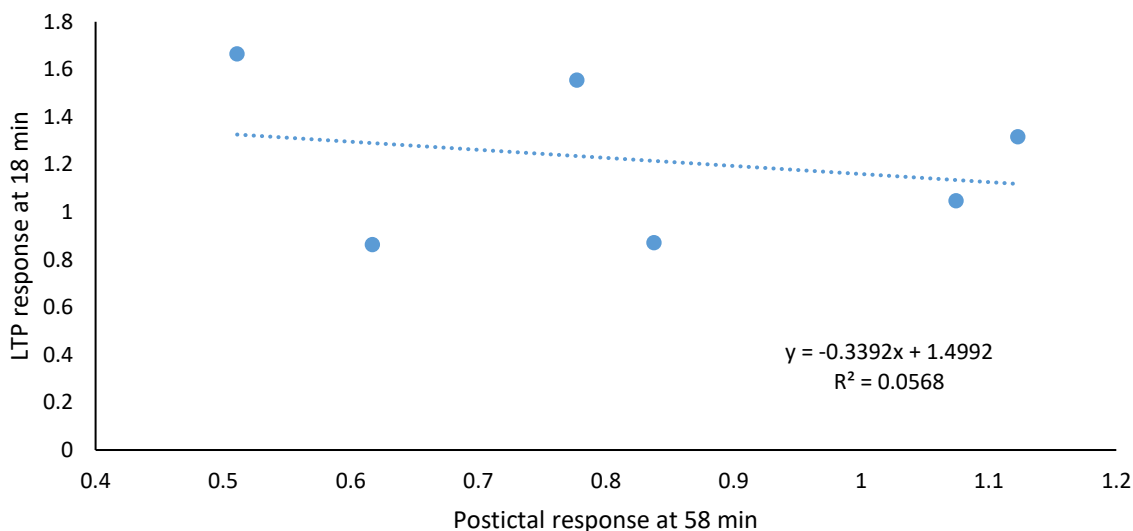


Fig 3.12. A graphical representation of LTP response at 18 min post-TBS (y) with postictal response at 60 min post-AD (x). The dotted trace was the best line fit with linear regression analysis, showing the equation for the line and goodness of fit R^2 . Each point indicates results from one animal.

Part II – Acute experiments

3.3 Responses in urethane-anesthetized mice

The relation between LTP and AD was further studied in wild-type (WT) and knockout (KO) urethane-anesthetized mice; there was no difference in the LTP and their response to AD, thus the data were grouped together. The urethane-anesthetized preparation allowed placement of multichannel electrodes for more precise study of the electrophysiological responses. Paired-pulses were used in all experiments, and the slope response to the first pulse will be called E1,

slope response to the second pulse will be called E2, and paired-pulse facilitation will be measured as the ratio of E2 to E1 ($E2/E1$).

A representative experiment illustrates basal dendritic response in CA1 before and after a 5-s high-frequency stimulation, which resulted in no AD (Fig 3.13). The response declined in the first 10 min, then showed signs of returning to baseline levels at ~1 h. At 1 hour post-AD, TBS of 4 sweeps each with 10 trains of theta-frequency bursts was applied to the cCA3 electrode to induce LTP in the CA1 region, followed by recording responses for another 2 h (Fig 3.13). The intensity used for tetanic stimulation ranged from 40 to 80 μ A, which was 2 times the threshold of a single-pulse response, and was always below that required to induce an AD. The response recovered to near baseline values before TBS. Following TBS, the basal dendritic response slope increased and showed robust LTP for the duration of the experiment (Fig 3.13).

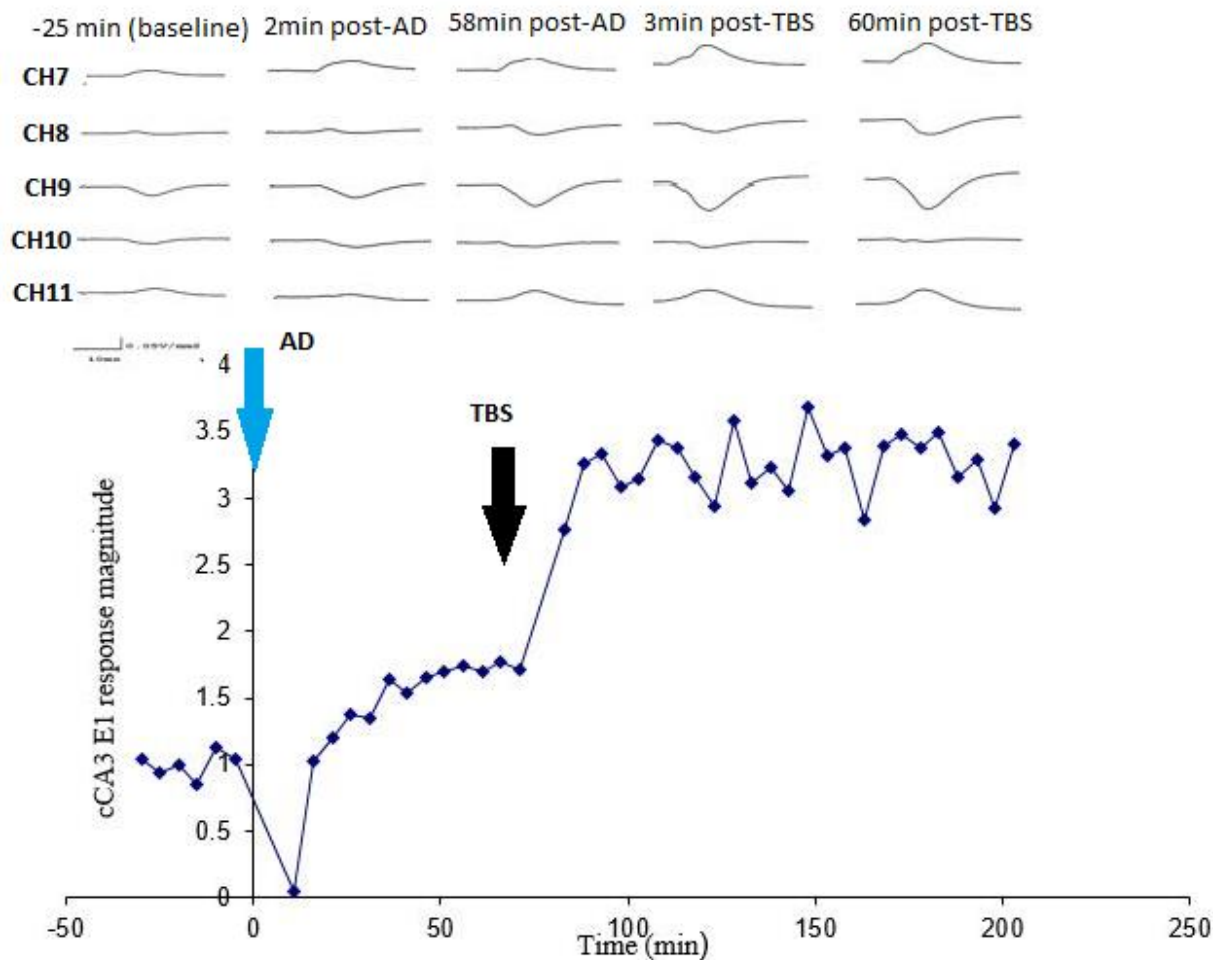


Figure 3.13. Data from a representative experiment (RG70) where high-frequency stimulation did not evoke an AD at time zero (blue arrow), after a 30-min baseline, followed by TBS (LTP induction; black arrow) at time 67 min. Normalized slope response to the first pulse (E1) at stratum oriens of CA1 in a representative mouse (RG70). A high-frequency stimulus (5 s of 100 Hz at 500 μ A) was applied at time 0 to iCA3 electrode, evoking an AD of 0 s duration; TBS was applied at 80 μ A to cCA3 electrode at 67 min post-AD. Top traces show CSD laminar profile at various time points throughout the course of the experiment; channel 9, showing maximal basal dendritic response, was analyzed.

Another experiment illustrates basal dendritic response in CA1 before and after HFS that resulted in an AD of 4.5s (Fig 3.14). The response declined in the first 10 min after the AD, and then showed signs of returning to baseline levels at \sim 1 h. At 1 hour post-AD, TBS of 4 sweeps each with 10 trains of theta-frequency bursts was applied to the cCA3 electrode to induce LTP in the CA1 region, followed by recording responses for another 2 h (Fig 3.14). The intensity used for

tetanic stimulation ranged from 40 to 80 μA , which was 2 times the threshold, and was always below that required to induce an AD. Following TBS, the basal dendritic response slope was not changed much, and showed a gradual decrease for the duration of the experiment (Fig 3.14).

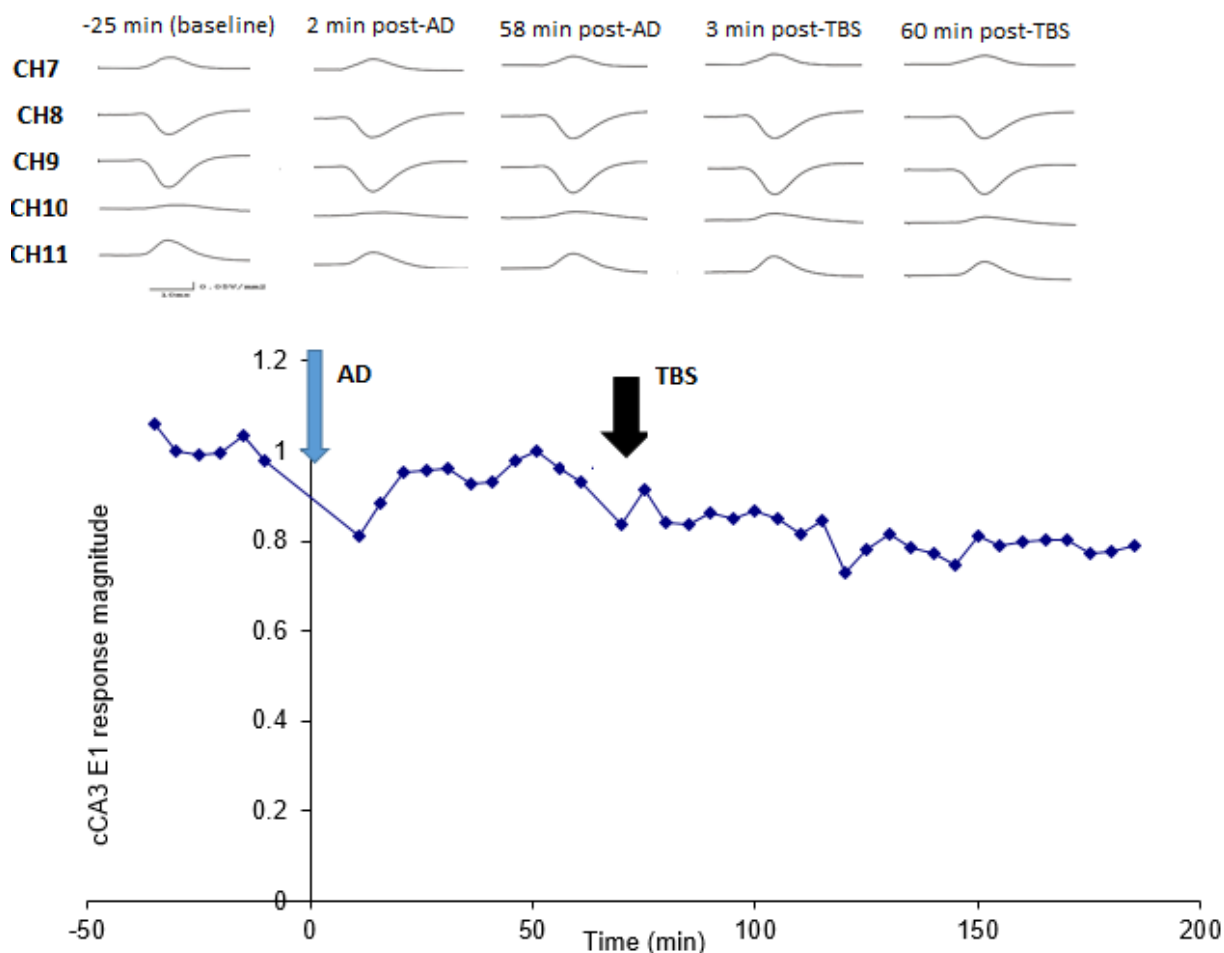


Figure 3.14. Data from a representative experiment (RG87) where an AD of 4.5s was evoked at time zero (blue arrow), after a 30-min baseline, followed by TBS (LTP induction; black arrow) at time 60 min. Normalized slope response to the first pulse (E1) at stratum oriens of CA1 in a representative mouse (RG87). A high-frequency stimulus (5 s of 100 Hz at 500 μA) was applied at time 0 to iCA3 electrode, evoking an AD of 4.5 s duration; TBS was applied at 80 μA to cCA3 electrode at 67 min post-AD. Top traces show CSD laminar profile at various time points throughout the course of the experiment; channel 9, showing maximal basal dendritic response, was analyzed.

3.3.1 AD duration vs LTP

Urethane anesthetic had a suppressive effect in evoking an AD. Thus, despite using a long stimulation (100-Hz) train of 5 s duration, an AD was only evoked in 6 of 12 mice, with AD duration varying from 4.5 to 15 s. In 6 of 12 mice, no AD was evoked (AD duration = 0). At least one channel of hippocampal EEG in CA1 was recorded on a polygraph machine during an AD (Fig 3.15).

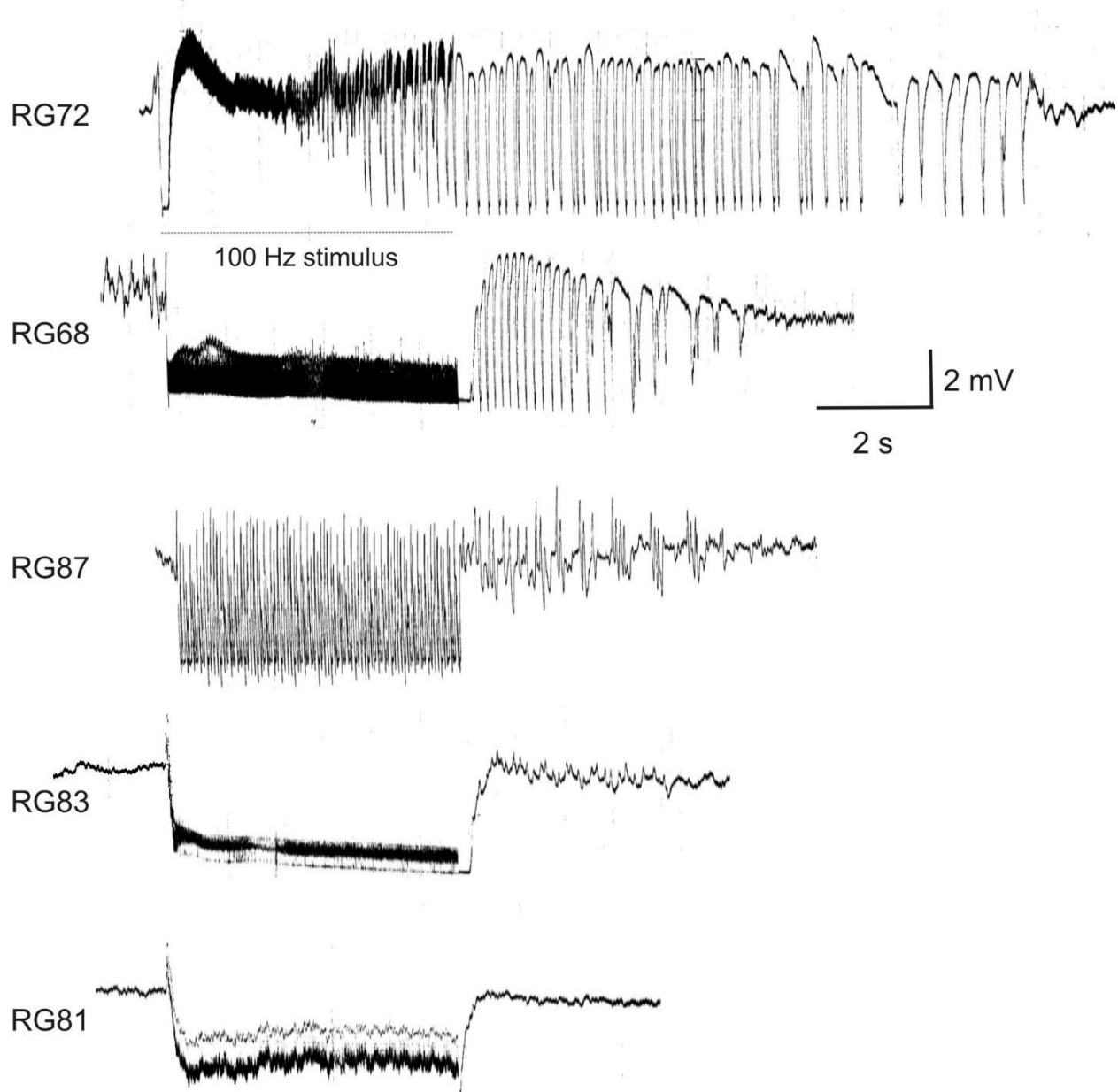


Figure 3.15. Electrophysiological activity at a CA1 distal dendritic electrode of selected experiments, before and after high-frequency (5 s of 100 Hz at 500 μ A) stimulation with the longest AD duration (RG72, 15 s) at the top and no AD duration at the bottom (RG81, 0 s). RG68 and RG87 had AD duration of 6 s and 4.5 s respectively. RG83 and RG81 had AD duration of 0 s. Figure made by Leung, L.S.

The relation between the post-TBS response and AD duration is shown in a scatter plot of all the mice, with each mouse represented by one point, and subjected to regression analysis (Fig. 3.16).

For the cCA3 pathway, a negative correlation was found between post-TBS response, recorded at 20 min after TBS, and AD duration (Fig. 3.16; $R^2 = 0.335$). The negative slope between the post-TBS response and AD duration was significantly different from zero ($F_{1,10} = 5.04$, $p = 0.048$). For the iCA3 pathway, there was a non-significant correlation between post-TBS response (recorded at 20 min after TBS) and AD duration (Fig 3.17; $R^2 = 0.075$; $F_{1,9} = 0.73$, $p = 0.4$). One mouse was excluded from the iCA3 analysis, as it did not show the typical basal dendritic response. It is noted that the tetanic stimulation (TBS) was only delivered to cCA3, and other than minor cross stimulation, the iCA3 pathway was not tetanized. Thus, there was little LTP in the iCA3-evoked response post-TBS.

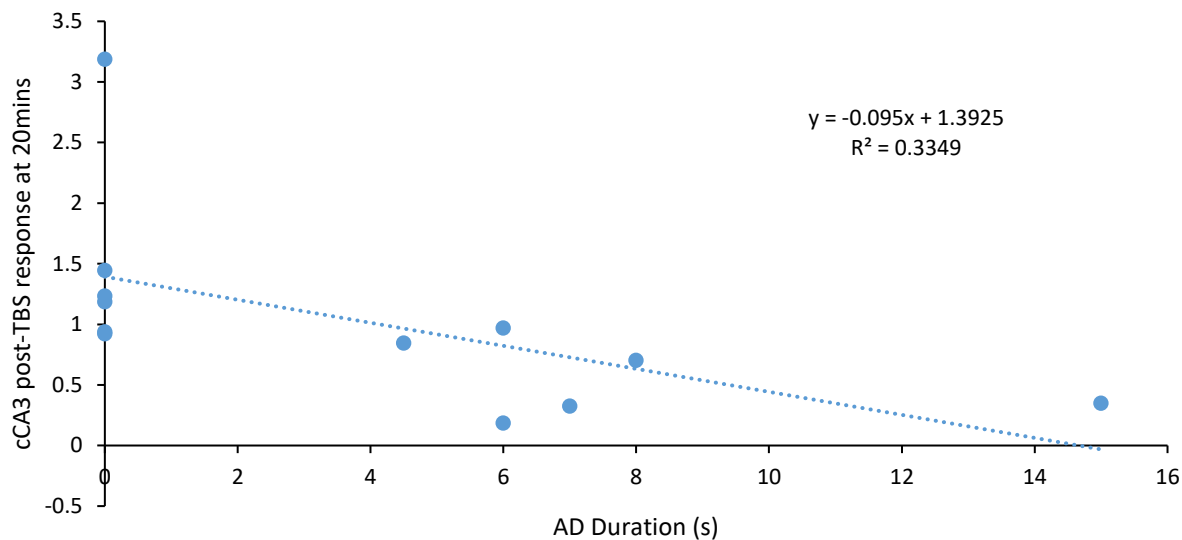


Figure 3.16. A plot of the cCA3 evoked post-TBS response at 20 min post-tetanus (y) with the AD of 0-15s duration (x) evoked one hour before tetanus (TBS). The dotted trace was the best line fit with linear regression analysis, showing the equation for the line and goodness of fit R^2 . Each point indicates results from one animal.

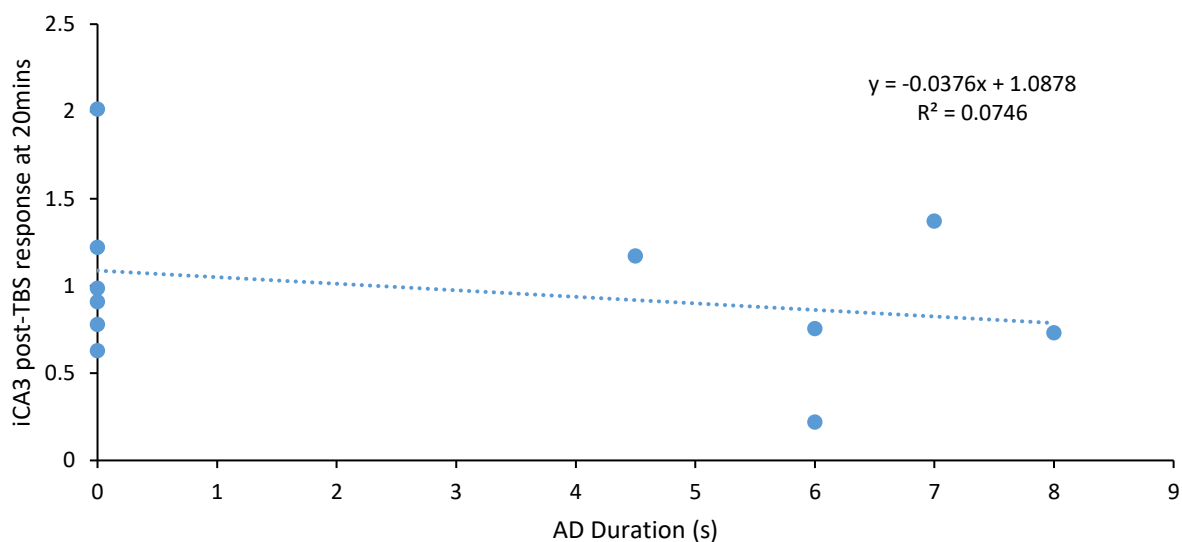


Figure 3.17. A plot of the iCA3 evoked post-TBS response at 20 min post-tetanus (y) with the AD of 0-8s duration (x) evoked one hour before tetanus (TBS). One mouse with 15s duration was excluded as it did not show a basal dendritic response in the iCA3 pathway. The dotted trace was the best line fit with linear regression analysis, showing the equation for the line and goodness of fit R^2 . Each point indicates results from one animal.

3.3.2 AD duration vs postictal response

Scatter plot and regression analysis were also used to analyze the relation between AD duration and postictal depression, for both the cCA3 and iCA3 pathways. The postictal response for the cCA3 pathway, in particular for 30-60 min post AD, generally decreased with AD duration (Fig 3.18). At 58 min post-AD, the postictal response showed a significant negative relationship ($R^2 = 0.3679$; $F_{1,10} = 5.82$, $p = 0.0365$) with the AD duration (Fig. 3.18). The postictal response for the iCA3 pathway, measured for 60 min post-AD, was not well fitted with a linear model, and at 58 min post-AD, showed no significant linear correlation ($R^2 = 0.0336$; $F_{1,9} = 0.31$, $p = 0.58$) with the AD duration (Fig 3.19).

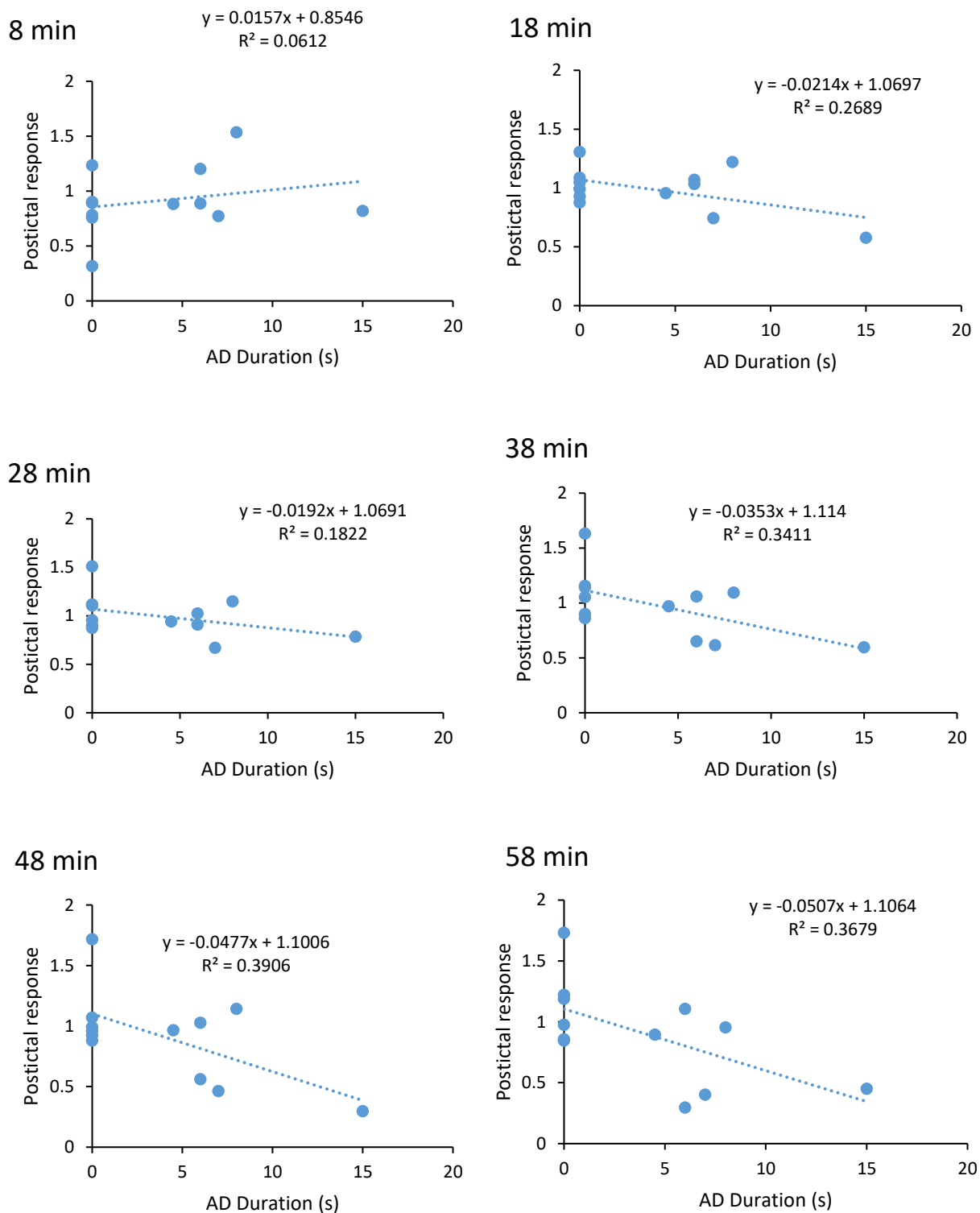


Figure 3.18. A series of graphs depicting the relation between cCA3 postictal response (y) (normalized by average baseline response) to AD duration (x) at different times after the AD for a group of 12 mice. Each point indicates result from one animal. Postictal responses at times 8, 18,

28, 38, 48, 58 min after the AD are plotted. Linear models were used to depict the relationship between the variables.

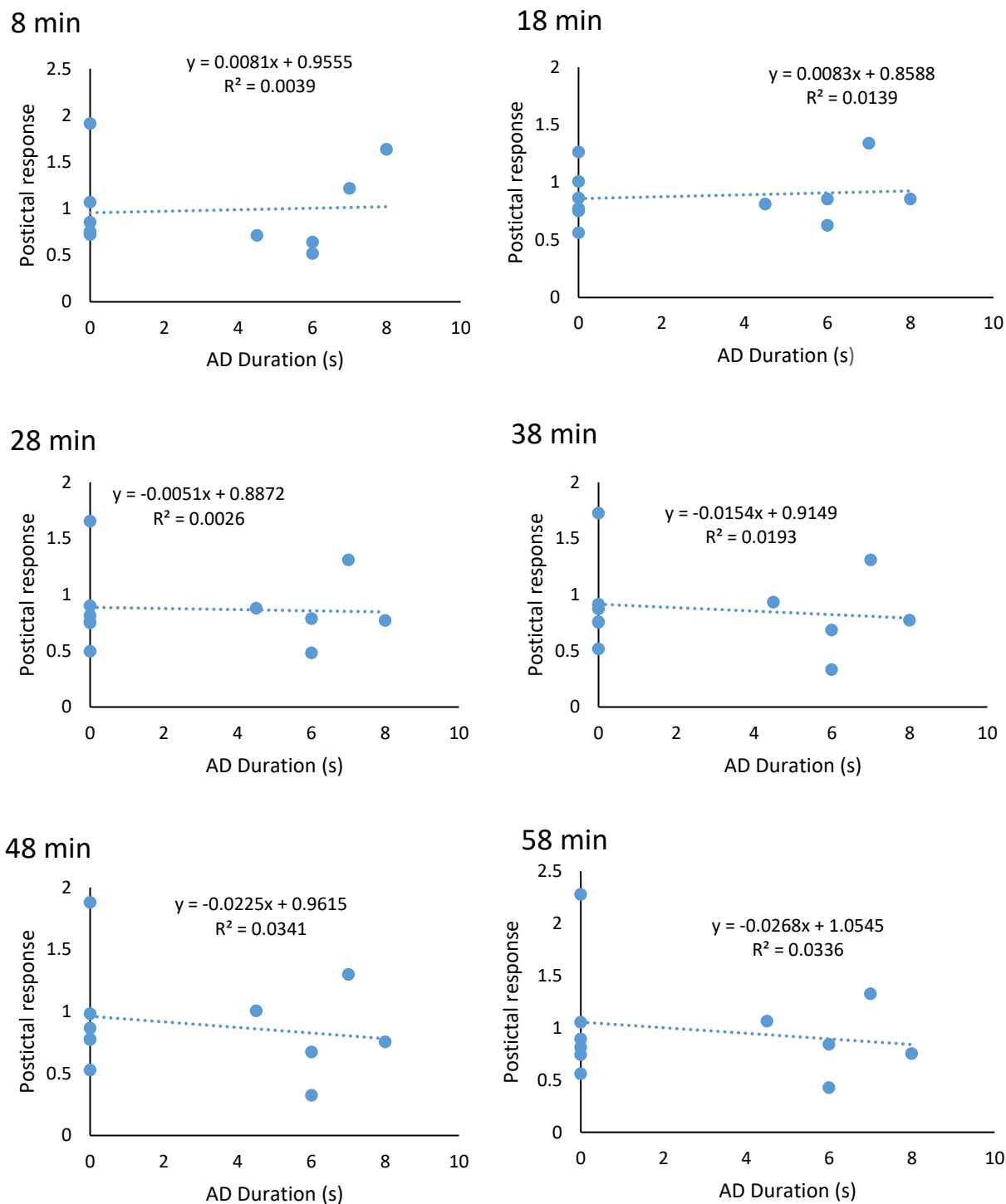


Figure 3.19. A series of graphs depicting the relation between iCA3 postictal response (y) (normalized by average baseline response) to AD duration (x) at different times after the AD for a

group of 12 mice. Each point indicates result from one animal. Postictal response at times 8, 18, 28, 38, 48, 58 min after the AD. Linear models were used to depict the relationship between the variables.

3.3.3 Postictal response vs LTP

Regression analysis was also used to correlate, among different mice, the postictal response at 60 min following AD to the LTP; LTP was evaluated at 10 min and 20 min following TBS. This comparison was done for the cCA3 pathway (contralateral to side of AD) and for the iCA3 pathway (ipsilateral to side of AD). For the cCA3 pathway, there was a positive linear relationship between LTP response at 10 min post-TBS and postictal response ($R^2 = 0.8141$; Fig. 3.20A), and the slope of the relation was significantly different from zero ($F_{1, 10} = 43.9$, $p < 0.01$). The same holds for the relationship between LTP response at 20 min post-TBS and postictal response as well ($R^2 = 0.832$; Fig 3.20B), and the slope of the relation was significantly different from zero ($F_{1, 10} = 49.5$, $p < 0.01$). For the iCA3 pathway, there appeared to be a positive linear relationship between the response at 10 min post-TBS and postictal response ($R^2 = 0.9316$; Fig. 3.21A) and the slope of the relation was significantly different from zero ($F_{1, 9} = 122.5$, $p < 0.01$). The trend held for the relationship between LTP response at 20 min post-TBS and postictal response as well ($R^2 = 0.9245$; Fig 3.21B) and the slope of the relation was significantly different from zero ($F_{1, 9} = 110.2$, $p < 0.01$).

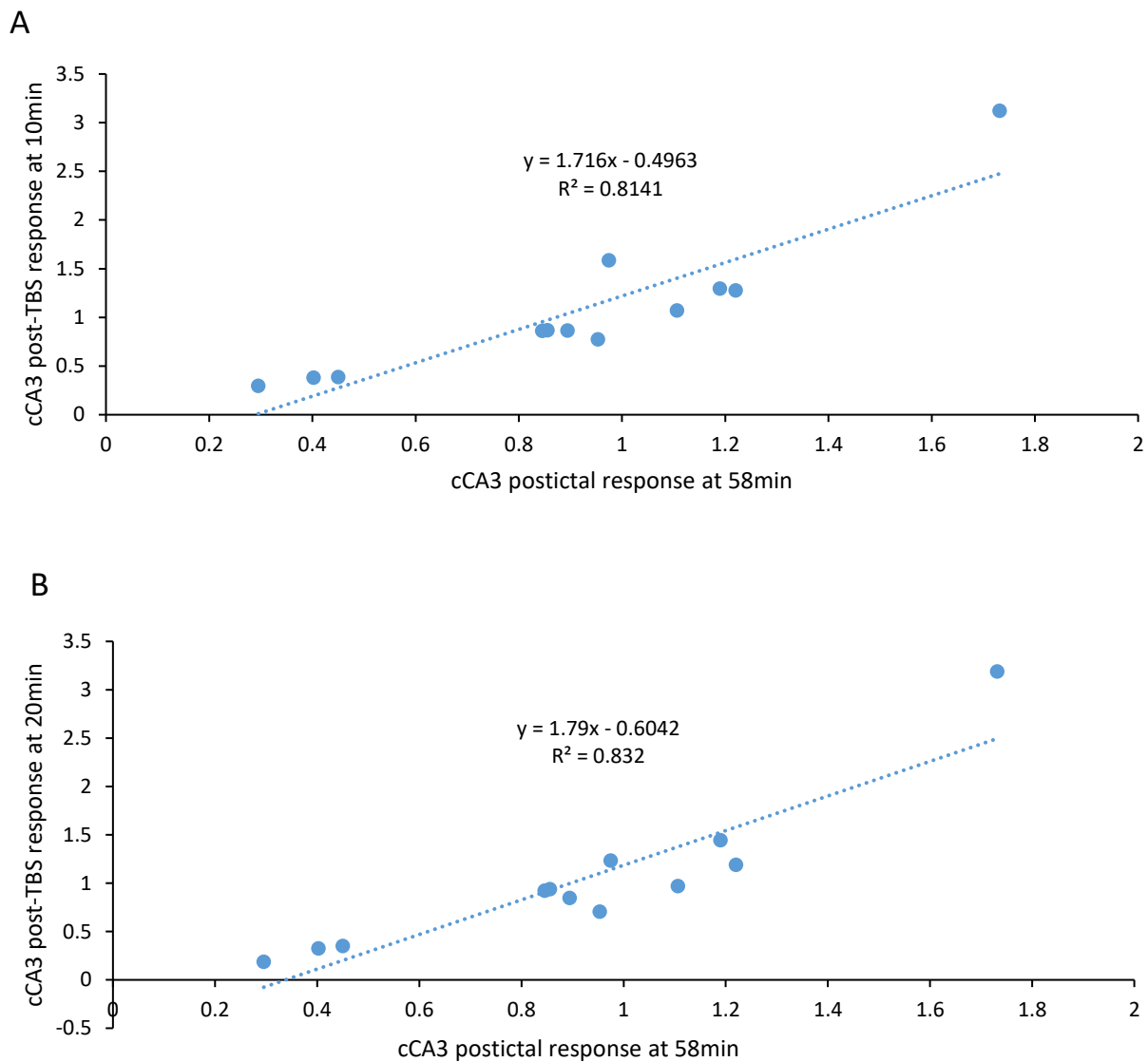


Figure 3.20. Plot of cCA3 LTP response at (A) 10 min and (B) 20 min post-TBS (y) with cCA3 postictal response at 60 min post-AD (x). The dotted trace was the best line fit with linear regression analysis, showing the equation for the line and goodness of fit R^2 . Each point indicates results from one animal.

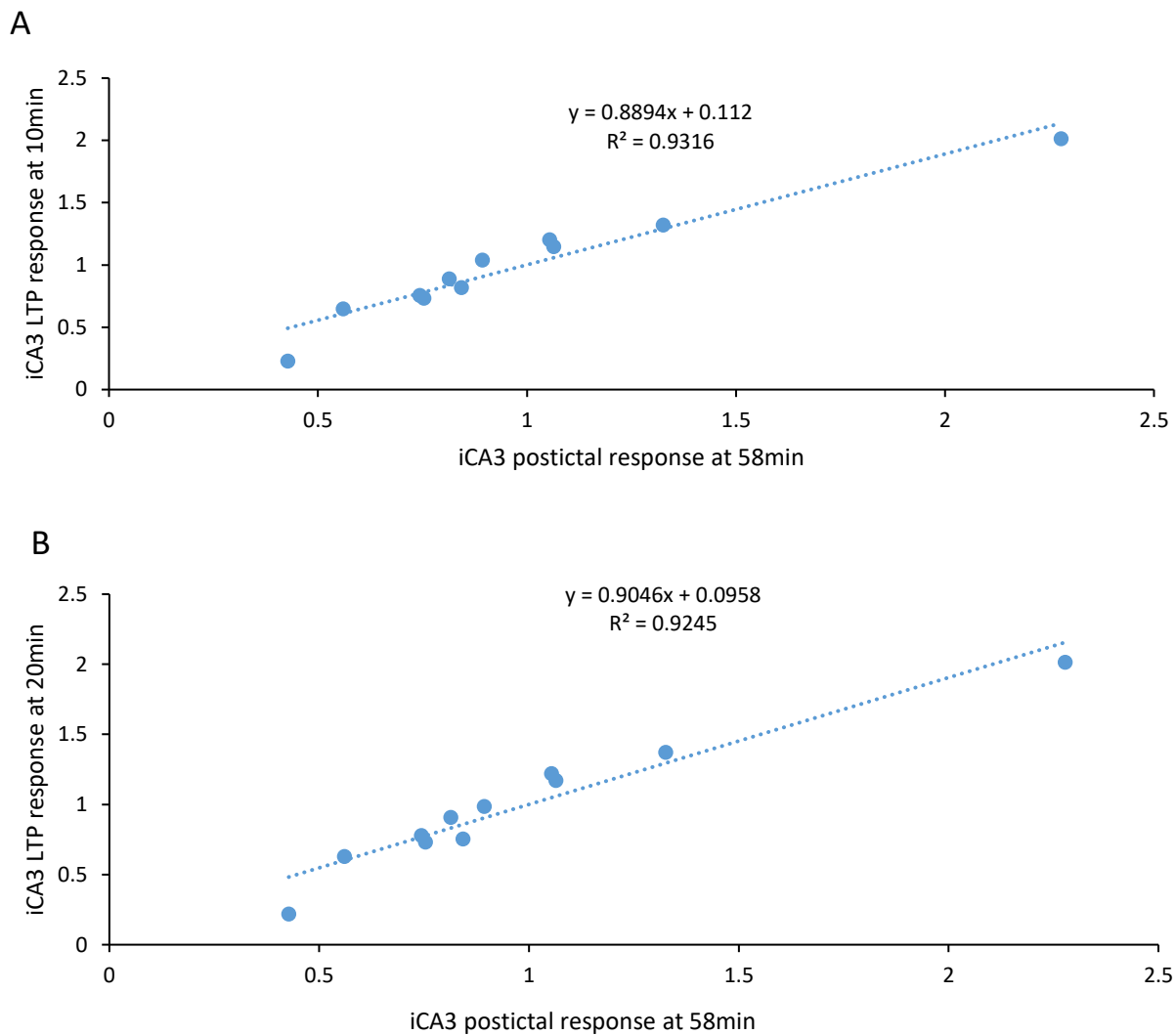


Figure 3.21. Plot of iCA3 LTP response at (A) 10 min and (B) 20 min post-TBS (y) with cCA3 postictal response at 60 min post-AD (x). The dotted trace was the best line fit with linear regression analysis, showing the equation for the line and goodness of fit R^2 . Each point indicates results from one animal.

3.3.4 Group analysis of the effect of an AD on postictal response

To show the effect of a long AD on postictal response, results were grouped into a no-AD group (AD duration = 0 s, n = 6 mice), and an AD group in which AD ranged from 4.5-15 s (n = 6 mice). Postictal responses were assessed by the slope response evoked by the first pulse (E1) and the second pulse (E2), and the ratio between the slope of the second pulse to the slope of the first pulse (E2/E1) for both the cCA3 pathway as well as the iCA3 pathway (Fig 3.22). In all conditions, the no-AD group showed apparent depression immediately following the 100 Hz high-frequency stimulation. While the AD group also showed depression post-HFS, the E2/E1 ratio for the iCA3 pathway showed an enhancement in response; hence, a repeated-measures two-factor ANOVA was conducted to investigate the effects of treatment and time on response. For the E1 response to cCA3 stimulation (Fig 3.22A), a repeated-measures two-factor ANOVA showed a significant interaction effect ($F_{9,100} = 3.79$, $p_{\text{interaction}} < 0.01$) without a significant main treatment effect ($F_{1,100} = 0.423$, $p_{\text{treatment}} = 0.528$) or significant effect of time ($F_{9,100} = 0.691$, $p_{\text{time}} = 0.715$). Further examination using a post hoc Newman-Keuls test revealed no significant differences between any time points. For the E2 cCA3 response (Fig 3.22B), a repeated-measures two-factor ANOVA showed no significant treatment effect ($F_{1,100} = 1.79$, $p_{\text{treatment}} = 0.211$) but a significant interaction effect ($F_{9,100} = 5.04$, $p_{\text{interaction}} < 0.01$) and time effect ($F_{9,100} = 2.60$, $p_{\text{time}} = 0.01$), with Newman-Keuls post hoc test showing significant differences between early (3-13 min) and late time points (43-48 min; see figure 3.21B). However, the repeated-measures two-factor ANOVA for the E2/E1 cCA3 response (Fig 3.22C) showed non-significant main, time, and interaction effects ($F_{1,100} = 2.81$; $p_{\text{treatment}} = 0.125$; $F_{9,100} = 1.91$, $p_{\text{time}} = 0.061$; $F_{9,100} = 0.292$, $p_{\text{interaction}} = 0.975$). For the iCA3 responses, there was no significant differences between no-AD and AD groups for E1 (Fig 3.22D; $F_{1,90} = 0.002$, $p_{\text{treatment}} = 0.968$; $F_{9,90} = 0.884$, $p_{\text{time}} = 0.543$; $F_{9,90} = 0.654$, $p_{\text{interaction}} = 0.747$), E2 (Fig 3.22E; $F_{1,90} = 0.252$, $p_{\text{treatment}} = 0.628$; $F_{9,90} = 1.05$, $p_{\text{time}} = 0.411$; $F_{9,90} = 0.430$, $p_{\text{interaction}} = 0.915$)

and E2/E1 iCA3 response (Fig 3.22F; $F_{1,90} = 2.20$, $p_{\text{treatment}} = 0.173$; $F_{9,90} = 0.841$, $p_{\text{time}} = 0.581$; $F_{9,90} = 0.741$, $p_{\text{interaction}} = 0.670$ repeated-measures two-factor ANOVA).

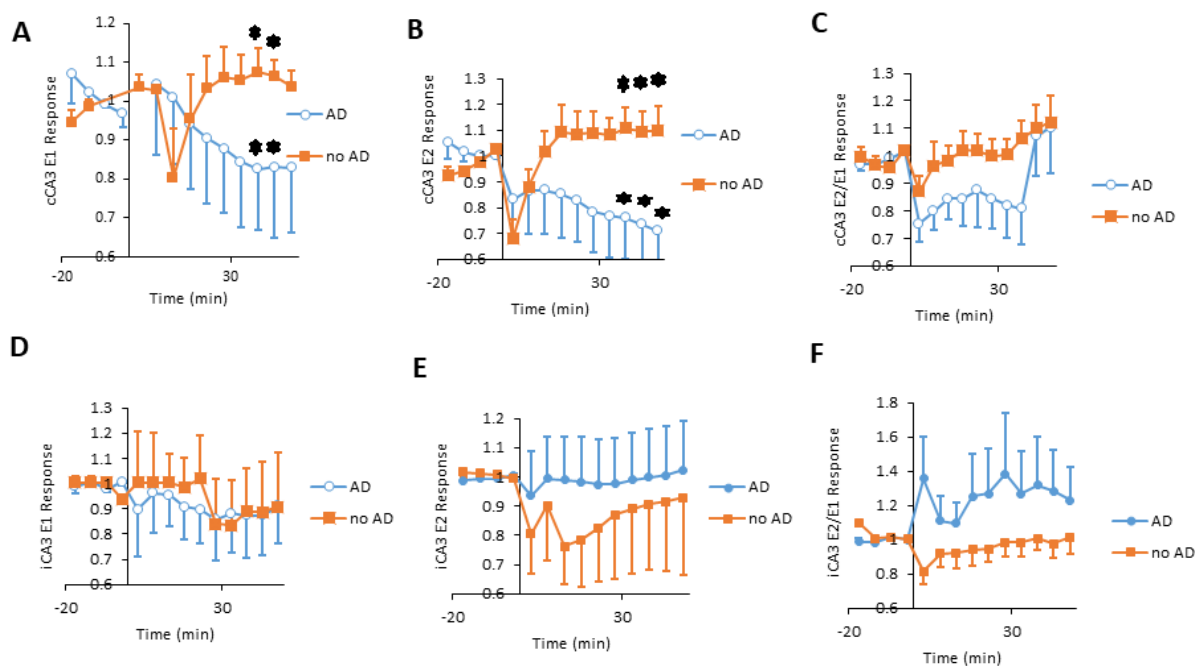


Figure 3.22. Postictal responses for no-AD and AD groups, showing mean and SEM of E1, E2 and E2/E1 across the duration of 8 min -58 min post-AD; each response was normalized by the average pre-AD baseline (-25 to -10 min pre-AD). High-frequency stimulation evoking AD or no AD was delivered to iCA3. A-C, responses of the cCA3 pathway, and D-F responses of iCA3 pathway. (A) shows normalized slope response to the first pulse (E1) evoked by cCA3 stimulation (B) shows normalized slope responses to the second pulse (E2) following cCA3 stimulation. (C) shows normalized response for the ratio between the second pulse slope and the first pulse slope (E2/E1) for the cCA3 pathway. (D) normalized E1 for the iCA3 pathway. (E) normalized E2 for the iCA3 pathway. (F) shows normalized E2/E1 ratio for the iCA3 pathway. All error bars shown depict standard error of the mean. Time points with an asterisk (*) are significantly different between no-AD and AD groups, using Newman-Keuls post hoc test.

3.3.5 Group analysis of the effect of an AD on LTP

The effect of an AD on LTP was also analyzed by a no-AD group (AD duration = 0 s, n=5 mice) and an AD group (AD duration 4.5-15 s, 6 mice). One mouse was excluded from the no-AD group because of missing data after 40 min post-TBS due to technical difficulties. Mean responses were calculated for the slope response magnitude evoked by the first pulse (E1), and of the second pulse (E2), and the ratio between the slope of the second pulse to the slope of the first pulse, respectively, after TBS stimulation for both the cCA3 as well as the iCA3 pathway (Fig 3.23). For the E1 cCA3 response (Fig 3.23A), a repeated-measures two-factor ANOVA revealed a significant main treatment effect ($F_{1,189} = 6.53$, $p_{\text{treatment}} = 0.031$). Newman-Keuls post hoc test revealed significant differences between almost all matching time points. Similarly, for the E2 cCA3 response (Fig 3.23B), a repeated-measures two-factor ANOVA revealed a significant main effect ($F_{1,189} = 10.5$, $p_{\text{treatment}} = 0.01$), with Newman-Keuls post hoc test showing significant differences between all matching time points, except for the latest time points. The E2/E1 cCA3 response (Fig 3.23C) also showed a significant main effect ($F_{1,189} = 5.48$, $p_{\text{treatment}} = 0.044$), with post hoc Newman-Keuls test showing significant differences between time points at middle and late times. For the iCA3 responses, there was no significant differences between no-AD and AD groups for E1 (Fig 3.23D; $F_{1,168} = 0.344$, $p_{\text{treatment}} = 0.573$; $F_{20,168} = 0.513$, $p_{\text{interaction}} = 0.958$), and E2 (Fig 3.23E; $F_{1,168} = 0.001$, $p_{\text{treatment}} = 0.979$; $F_{20,168} = 0.183$, $p_{\text{interaction}} = 1$). However, the E2/E1 iCA3 response (Fig 3.23F) showed a significant interaction effect ($F_{20,168} = 1.68$, $p = 0.042$), with a post hoc Newman-Keuls test showing significant differences at mid- and late time points.

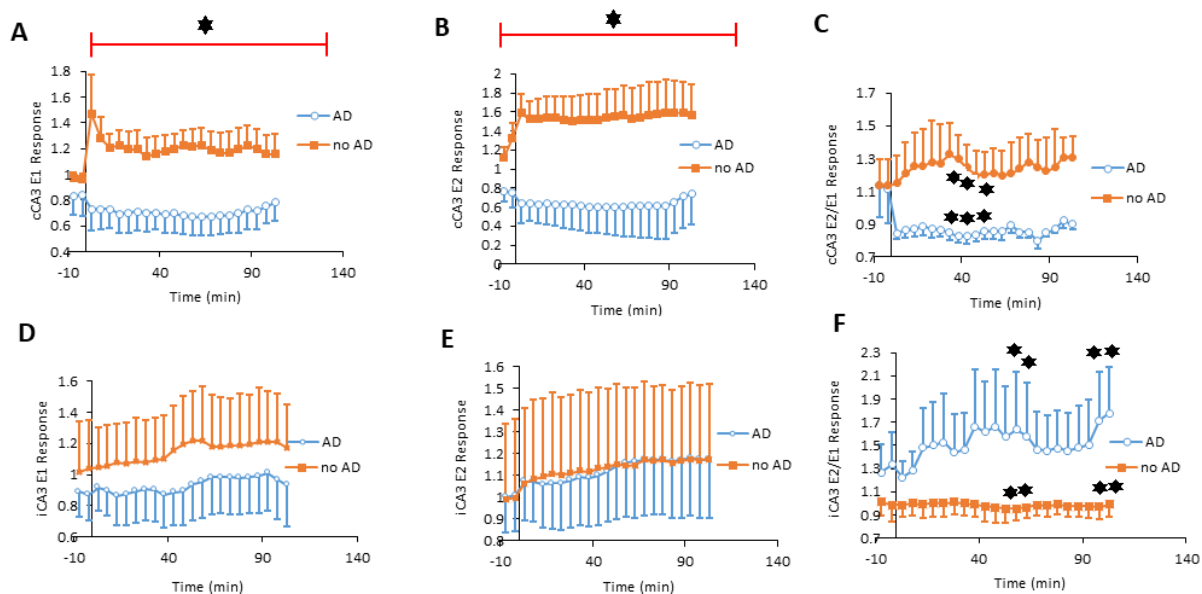


Figure 3.23. Responses after theta-burst stimulation (TBS) in no-AD and AD groups, showing mean and SEM of E1, E2 and E2/E1 across all post-TBS time points, and two time points before TBS (53 and 58min post-AD). TBS was delivered to the cCA3 electrode at 63 min after HFS that evoked AD or no AD. Responses were normalized by the average baseline response before HFS. A-C, responses of the cCA3 pathway, and D-F responses of iCA3 pathway. (A) shows normalized slope responses to the first pulse (E1) of cCA3 stimulation. (B) shows normalized slope responses to the second pulse (E2) after cCA3 stimulation. (C) shows normalized E2/E1 ratio after cCA3 stimulation. (D) normalized E1 for the iCA3 pathway. (E) normalized E2 for the iCA3 pathway. (F) shows normalized E2/E1 ratio for the iCA3 pathway. Error bars indicate standard error of the mean response. Time points with an asterisk (*) are significantly different between no-AD and AD groups, using Newman-Keuls post hoc test.

3.2.11 Group analysis of primed burst tetanus

To determine if there was a difference in the responses during TBS, slope responses were measured during the TBS for the no-AD group and AD groups described above, except one mouse was excluded from the AD group because its burst responses were not properly recorded due to a technical glitch. The slope of the potential recorded at stratum oriens was analyzed after the first pulse of each of the 4 traces of the TBS, and normalized by the first-pulse, first-trace response (Fig 3.24). A repeated-measures two-factor ANOVA revealed non-significant treatment ($F_{1,27} = 0.997$, $p_{\text{treatment}} = 0.344$) and treatment x time interaction effects ($F_{2,27} = 1.62$, $p_{\text{interaction}} = 0.223$). There was no short-term potentiation revealed by the present analysis, and the slight increase in mean response magnitude for the 2nd and 3rd traces of the AD group was not found to be statistically significant ($p_{\text{time}} > 0.2$)

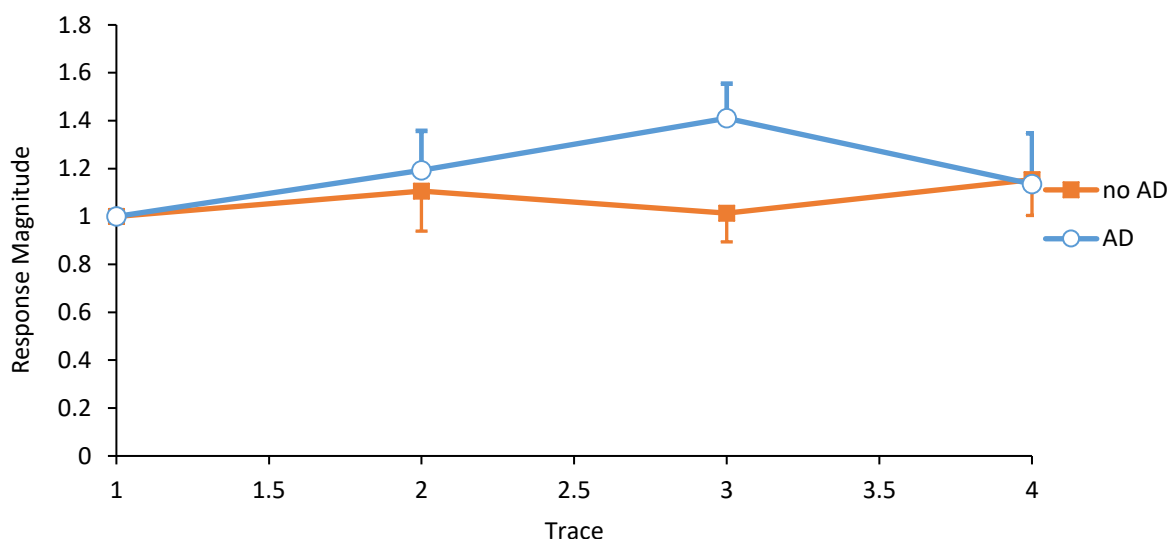


Figure 3.24. Group average of no-AD and AD groups, showing mean and SEM of the response to the first pulse of across all 4 traces applied during TBS. Responses were normalized by the response to the first pulse of the first trace. Each trace or train consisted of 10 theta-frequency bursts; each burst was 100 pulses at 100 Hz separated from each other by 200 ms.

Chapter 4: Discussion

4.1 Main Results

Through both chronic and acute paradigms, this study had produced original data exploring the relationship between an AD and LTP response magnitude. In freely behaving mice, we showed that LTP was suppressed if an AD was induced one hour earlier, and these suppressive effects lasted about 30 min after LTP induction, irrespective of mouse genotype. In all mice under urethane anesthesia, we found that LTP was completely abolished if induced 1 h after an AD, when compared to a group without prior AD. A longer AD duration was found to result in larger postictal depression.

4.2 AD, postictal response, and LTP in chronic behaving mice paradigm

In freely behaving mice, we found that LTP was suppressed by an AD induced at 1 hour before the AD, but not at 1 day or 1 week before the AD. Studying AD-LTP intervals of one day or longer was only possible in behaving mice, since *in vitro* preparations could not test AD-LTP intervals of more than several hours (Barr et al., 1997; Moore et al., 1993). The paradigm also made it possible to observe behavioural changes during stimulation. Eliciting an AD caused the mouse to momentarily remain stationary while maintaining an alert posture, whereas the TBS used to elicit LTP did not elicit any behavioural effects.

For behaving mice, a non-significant positive correlation was found between AD duration and LTP response magnitude at 20 min post-TBS; LTP was induced at 1 h post-AD. This result was surprising as longer AD duration was expected to correlate with lower LTP response magnitude (Barr et al., 1997), i.e., a negative correlation. This discrepancy could be attributed to the small sample size.

Postictal response and AD duration showed an inverse quadratic relation, indicating that postictal depression could be seen at short (2 s) and long (32 s) AD durations. A 2-s AD duration from a VACHT knockout (KO) mouse was found to result in unexpectedly strong postictal depression. It should also be noted that with each progressive time point, the quadratic relationship between AD and postictal response weakened, and postictal depression mainly recovered at 58 min post-AD. Postictal response magnitude at 58 min post-AD was not significantly correlated to the LTP magnitude (measured at 20 min post-TBS) induced at 1 h post AD.

A limitation in the study on behaving mice is that different strains of mice were used for the study, and the total sample size was small. The limitation in the number of behaving mice that could be used was beyond the control of our laboratory.

4.3 AD, postictal response, and LTP in acute urethane-anesthetized mice paradigm

Acute, urethane-anesthetized mice were used to examine the detailed relationship between AD, postictal response, and LTP. This procedure also made it possible to use a 16-channel probe to collect data from various depth of the CA1, and CSD analysis to reduce the effect of volume conduction.

The relationship between postictal response and AD duration in urethane-anesthetized mice was somewhat different from that found in behaving mice. In urethane anesthetized mice, AD was induced by stimulation at the iCA3 electrode, while the cCA3 pathway was used to induce LTP. For the cCA3 evoked responses, the 58 min post-AD response was significantly correlated with AD duration, such that low postictal responses were associated with long AD durations. However, there was no significant linear relationship seen for the iCA3 evoked responses and AD duration. For most mice, the iCA3 evoked responses remained low regardless of AD duration, perhaps

suggesting that the high frequency stimulation and AD had a suprathreshold and very strong neuronal silencing effect on the iCA3 evoked responses. It should be noted that some mice showed postictal potentiation of the iCA3 evoked responses after an AD, which typically lasted only for 30 min.

Urethane anesthetic had a suppressive effect in evoking an AD, as was observed in other studies (Cain et al., 1993). Thus, despite using a long stimulation of high intensity (100-Hz train of duration 5s), an AD was only evoked in 6 of 12 mice, with AD duration varying from 4.5 to 15 s, typically shorter than those in behaving animals. In the remaining 6 mice, no AD was evoked (AD duration = 0). Group analysis of the postictal response period showed a significant relationship of the postictal response to AD duration for the responses evoked by cCA3 stimulation but not those evoked by iCA3 stimulation. Specifically, the cCA3 evoked E1 and E2 responses showed significant differences between the two groups for later postictal time points, indicating that the application of an AD leads to persistent postictal depression. The lack of significant correlation of the iCA3 evoked E1 and E2 responses and AD duration could very well be explained by the fact the high-frequency stimulation or a minimal AD (of short duration) would strongly suppress iCA3 evoked responses.

When comparing postictal response magnitude at the time of recovery, which was 58 min post-AD, to LTP response magnitude at 20 min post-TBS, there was significant correlation for both pathways; this indicates that as postictal response increases after a state of depression, LTP response magnitude also increases with AD duration, which is in line with previous literature (Barr et al., 1997; Moore et al., 1993).

The relationship between AD duration and LTP was analyzed in both the cCA3 and iCA3 pathways. For the cCA3 pathway, the post-TBS response was negatively correlated with AD

duration such that lower response levels were associated with longer AD durations, which was expected (Barr et al., 1997). However, in the iCA3 pathway, the post-TBS response was not significantly correlated with AD duration. As expected for a non-tetanized pathway, post-TBS responses evoked by iCA3 stimulation are not expected to be altered. However, it is possible that there was a minor spread of stimulus currents to the afferents contributing to the iCA3 evoked responses during TBS of the cCA3 electrode. The relationship between AD duration and LTP in the urethane-anesthetized mice is in stark contrast with that in freely behaving mice, as the latter did not display a significant relationship. This could be attributed to the small sample size of the behaving mice used, and also larger variation of LTP because of lack of behavioral clamping during the experiment.

When examining the relationship between the LTP response magnitude in groups with or without an AD, the cCA3 responses showed significant group differences for E1 and E2, and E2/E1 for many matching time points. This supports our initial findings with the behaving mice that an AD of considerable duration leads to suppression of LTP response magnitude, and AD duration is an important factor to consider when examining the suppressive effects of an AD. The iCA3 pathway did not show any significant difference between AD and no-AD groups for the E1 and E2 responses after TBS; however, E2/E1 was significantly different for mid and late time points. As the present design of the experiment does not account for the possible effect of a 100 Hz stimulus that did not evoke an AD, a potential explanation might be that without the 100 Hz strong 5 s stimulation, E2/E1 after TBS would show a decrease. It should also be noted that for the acute experiments, control (WT) and ATRX knockout (KO) mice were assumed to be not different in their postictal and LTP responses. Post hoc analysis confirmed this assumption.

Group analysis of the responses during primed burst showed that there was no difference between the responses of the no-AD and AD groups. However, while the average responses during repeated primed bursts showed short-term potentiation (STP), it was not significant in either the AD or the no-AD group. Still, there was no STP difference between no-AD and AD groups.

4.4 Previous studies on AD vs LTP

Previous studies have investigated the relationship between AD and LTP response (Barr et al., 1987; Leung & Shen, 1993; Moore et al., 1993). Barr and colleagues used *in vitro* hippocampal slices to elicit an AD and attempted to elicit LTP at various time points post-AD in order to pinpoint the duration of AD suppression on LTP induction. They concluded that AD duration and postictal response was inversely proportional to LTP induction, such that long AD and postictal depression were correlated with suppression of LTP induction (Barr et al., 1997). AD duration was also directly proportional to postictal response such that postictal response levels were depressed for long AD durations (Barr et al., 1997). Suppression of postictal response and LTP by long AD durations was also found in the present study.

Leung & Shen (1993) used tetanic stimulation that evoked AD of different durations in freely behaving rats, which was followed by potentiation of basal dendritic fEPSPs. It was also concluded that potentiation following a single tetanic stimulation was smaller in experiments where ADs were longer than 15 s compared to those with ADs less than 15s (Leung & Shen, 1993). Leung & Shen (1993) used the same electrode to induce AD and LTP whereas the present paradigm consistently used different electrodes to induce AD and LTP. However, a suppression of LTP by a long ADs was also found in the present study. In addition, the present study showed a total lack of LTP after an AD, while all previous studies (Barr et al. 1997; Moore et al. 1993; Leung & Shen, 1993) showed reduced but not zero LTP.

The effect of an AD on LTP may be similar to that of an AD on memory impairment. Cain et al., (1993) showed that an AD led to memory impairments in a behavioural task close to the time of training but not for longer than one day; however, there was no correlation made between AD and synaptic plasticity to account for the mechanism for the memory impairment. Whether LTP suppression is a correlate of memory impairment requires further study.

4.5 Potential mechanisms of LTP suppression by an AD

Various studies have attempted to elucidate the mechanisms by which AD causes suppressive effects on neuronal responses, although few studies have suggested a mechanism on LTP. Computational models have identified that afterdischarges are associated with elevated extracellular K^+ concentration and decreased intracellular Na^+ concentration (Krishnan & Bazhenov, 2011; Kager et al., 2006). However, return of these ions to baseline levels is relatively quick and may not explain the suppression of LTP response.

One possible mechanism involves presynaptic calcium levels. Studies have shown that seizure activity has led to a decrease in extracellular Ca^{2+} concentration (Heinemann et al., 1977). Disruption of paired-pulse facilitation by an AD on iCA3 and cCA3 responses suggests that an AD disrupted presynaptic Ca^{2+} levels. Decreased extracellular Ca^{2+} may reduce the amount of Ca^{2+} influx during the induction of LTP. Since single-pulse responses were not abolished by an AD, reduction of presynaptic Ca^{2+} available for LTP had to be larger than that available for single-pulse evoked synaptic transmission. It was also reported that kindled animals had a permanent decrease in CaM kinase II activity, a major calcium-regulated transducing system (Perlin et al., 1992). Since CaM kinase II is needed for the recruitment of more AMPA receptors to the membrane (Kandel et al., 2014; Bliss et al., 2007), the expression of LTP may be diminished.

Another possible mechanism involves adenosine, a neuromodulator that can modulate or inhibit LTP and is released during synchronized firing during seizures; adenosine has also been associated with postictal depression (Barr et al., 1997; During & Spencer, 1992). Barr and colleagues (1997) used an adenosine antagonist to delay postictal depression during a period where LTP would normally be suppressed, and discovered that LTP induction was possible in the presence of this antagonist. Thus, the depression effects seen in this current study could be due to the release of adenosine, which effectively blocks LTP response.

NMDA receptors could also play a vital role in explaining the suppression of LTP via an AD. Stasheff and colleagues (1989) showed that an NMDA-antagonist blocks the ability to elicit an AD, while Leung & Shen (1993) showed that an NMDA-antagonist reduced AD duration significantly. Cornejo et al., (2007) found that a single neonatal seizure suppressed LTP in adult rats, and induced a decrease in the total amount of NMDA 2A receptors and the membrane pool of glutamate (AMPA) receptor 1 subunits. As both NMDA and AMPA receptors are important for LTP induction and maintenance, this reduction could lead to the LTP suppression observed in this study. Furthermore, NMDA receptor activation has been linked to adenosine release in the hippocampus; thus, NMDA receptor activation during seizure activity could contribute to adenosine release, as well, thus exacerbating the effect of adenosine on LTP response (Barr et al., 1997).

4.6 Future Studies

While this study has attempted to establish the relationship between AD and LTP, there was no examination of the detrimental effect an AD has on memory. Future research can expand on our study via inclusion of a memory paradigm in order to investigate the consequences of short-term suppression of LTP following an AD. Though our work has indicated that an AD has a suppressive

effect on LTP, the mechanism remains unclear; future research can aim to establish the mechanistic relationship between these two phenomena. While the mechanism and behavioural translation remains to be elucidated, this study has shown through both chronic and acute paradigms that LTP can be suppressed by an AD that was induced one hour earlier, with AD duration being an important factor that contributes to this suppression effect.

References

- Abraham, W. C., Mason-Parker, S. E., Bear, M. F., Webb, S., & Tate, W. P. (2001). Heterosynaptic metaplasticity in the hippocampus in vivo: A BCM-like modifiable threshold for LTP. *Proceedings of the National Academy of Sciences*, *98*(19), 10924-10929.
- Abraham, W. C., & Williams, J. M. (2003). Properties and Mechanisms of LTP Maintenance. *The Neuroscientist*, *9*(6), 463-474.
- Abraham, W. C. (2008). Metaplasticity: Tuning synapses and networks for plasticity. *Nature Reviews Neuroscience*, *9*(5), 387-387.
- Al-Onaizi, M. A., Parfitt, G. M., Kolisnyk, B., Law, C. S., Guzman, M. S., Barros, D. M., . . . Prado, V. F. (2017). Regulation of Cognitive Processing by Hippocampal Cholinergic Tone. *Cerebral Cortex*, *27*(2), 1615-1628.
- Anagnostaras, S. G., Murphy, G. G., Hamilton, S. E., Mitchell, S. L., Rahnema, N. P., Nathanson, N. M., & Silva, A. J. (2002). Selective cognitive dysfunction in acetylcholine M1 muscarinic receptor mutant mice. *Nature Neuroscience*, *6*(1), 51-58.
- Anwyl, R., Walshe, J., & Rowan, M. (1987). Electroconvulsive treatment reduces long-term potentiation in rat hippocampus. *Brain Research*, *435*(1-2), 377-379.
- Augustinack, J. C., Kouwe, A. J., Salat, D. H., Benner, T., Stevens, A. A., Annese, J., . . . Corkin, S. (2014). H.M.s contributions to neuroscience: A review and autopsy studies. *Hippocampus*, *24*(11), 1267-1286.
- Bach, M. E., Hawkins, R. D., Osman, M., Kandel, E. R., & Mayford, M. (1995). Impairment of spatial but not contextual memory in CaMKII mutant mice with a selective loss of hippocampal ltp in the range of the θ frequency. *Cell*, *81*(6), 905-915.
- Barnes, C., Jung, M., Mcnaughton, B., Korol, D., Andreasson, K., & Worley, P. (1994). LTP saturation and spatial learning disruption: Effects of task variables and saturation levels. *The Journal of Neuroscience*, *14*(10), 5793-5806.
- Barr, D. S., Hoyt, K. L., Moore, S. D., & Wilson, W. A. (1997). Post-ictal depression transiently inhibits induction of LTP in area CA1 of the rat hippocampal slice. *Epilepsy Research*, *27*(2), 111-118.
- Bi, G., & Poo, M. (2001). Synaptic Modification by Correlated Activity: Hebb's Postulate Revisited. *Annual Review of Neuroscience*, *24*(1), 139-166.
- Bliss, T. V., & Lømo, T. (1973). Long-lasting potentiation of synaptic transmission in the dentate area of the anaesthetized rabbit following stimulation of the perforant path. *The Journal of Physiology*, *232*(2), 331-356.

- Bliss, T. V., & Collingridge, G. L. (1993). A synaptic model of memory: Long-term potentiation in the hippocampus. *Nature*, *361*(6407), 31-39.
- Bliss, T., Collingridge, G., & Morris, R. (2007). Synaptic plasticity in the hippocampus. In P. Andersen, R. Morris, & D. Amaral (Authors), *The hippocampus book* (pp. 343-474). Oxford: Oxford University Press.
- Blitzer, R. D., Gil, O., & Landau, E. M. (1990). Cholinergic stimulation enhances long-term potentiation in the CA1 region of rat hippocampus. *Neuroscience Letters*, *119*(2), 207-210.
- Cain, D. P., Boon, F., & Hargreaves, E. L. (1992). Evidence for different neurochemical contributions to long-term potentiation and to kindling and kindling-induced potentiation: Role of NMDA and urethane-sensitive mechanisms. *Experimental Neurology*, *116*(3), 330-338.
- Cain, D. P., Hargreaves, E. L., Boon, F., & Dennison, Z. (1993). An examination of the relations between hippocampal long-term potentiation, kindling, afterdischarge, and place learning in the water maze. *Hippocampus*, *3*(2), 153-163.
- Capogna, M. (2011). Neurogliaform cells and other interneurons of stratum lacunosum-moleculare gate entorhinal-hippocampal dialogue. *The Journal of Physiology*, *589*(8), 1875-1883.
- Coan, E., Irving, A., & Collingridge, G. (1989). Low-frequency activation of the NMDA receptor system can prevent the induction of LTP. *Neuroscience Letters*, *105*(1-2), 205-210.
- Cornejo, B. J., Mesches, M. H., Coultrap, S., Browning, M. D., & Benke, T. A. (2007). A single episode of Neonatal Seizures Permanently Alters Glutamatergic Synapses. *Annals of Neurology*, *61*(5), 411-426.
- Deweert, B., Lehericy, S., Pillon, B., Baulac, M., Chiras, J., Marsault, C., . . . Dubois, B. (1995). Memory disorders in probable Alzheimers disease: The role of hippocampal atrophy as shown with MRI. *Journal of Neurology, Neurosurgery & Psychiatry*, *58*(5), 590-597.
- Doralp, S., & Leung, L. (2008). Cholinergic modulation of hippocampal CA1 basal-dendritic long-term potentiation. *Neurobiology of Learning and Memory*, *90*(2), 382-388.
- During, M. J., & Spencer, D. D. (1992). Adenosine: A potential mediator of seizure arrest and postictal refractoriness. *Annals of Neurology*, *32*(5), 618-624.
- Faure, A., Verret, L., Bozon, B., Tayara, N. E., Ly, M., Kober, F., . . . Delatour, B. (2011). Impaired neurogenesis, neuronal loss, and brain functional deficits in the APPxPS1-Ki mouse model of Alzheimers disease. *Neurobiology of Aging*, *32*(3), 407-418.
- Fox, S., & Ranck, J. (1975). Localization and anatomical identification of theta and complex spike

- cells in dorsal hippocampal formation of rats. *Experimental Neurology*, 49(1), 299-313.
- Freeman, J. A., & Nicholson, C. (1975). Experimental optimization of current source-density technique for anuran cerebellum. *Journal of Neurophysiology*, 38(2), 369-382.
- Gilbert, M., & Mack, C. (1990). The NMDA antagonist, MK-801, suppresses long-term potentiation, kindling, and kindling-induced potentiation in the perforant path of the unanesthetized rat. *Brain Research*, 519(1-2), 89-96.
- Green, J. D., & Petsche, H. (1961). Hippocampal electrical activity IV. Abnormal electrical activity. *Electroencephalography and Clinical Neurophysiology*, 13(6), 868-879.
- Halgren, E., Babb, T. L., & Crandall, P.H. (1978a). Activity of human hippocampal formation and amygdala neurons during memory testing. *Electroencephalography and Clinical Neurophysiology*, 45(5), 585-601.
- Halgren, E., Walter, R. D., Cherlow, D. G., & Crandall, P. H. (1978b). Mental Phenomena Evoked By Electrical Stimulation Of The Human Hippocampal Formation and Amygdala. *Brain*, 101(1), 83-115.
- Halgren, E., & Wilson, C. L. (1985). Recall deficits produced by afterdischarges in the human hippocampal formation and amygdala. *Electroencephalography and Clinical Neurophysiology*, 61(5), 375-380.
- Halliday, G. (2017). Pathology and hippocampal atrophy in Alzheimers disease. *The Lancet Neurology*, 16(11), 862-864.
- Hebb, D. O. (1949). The organization of behavior: A neuropsychological theory. *Science Education*, 34(5), 336-337.
- Heinemann, U., Lux, H., & Gutnick, M. (1977). Extracellular free calcium and potassium during paroxysmal activity in the cerebral cortex of the cat. *Experimental Brain Research*, 27-27(3-4), 237-243.
- Huang, Y., Colino, A., Selig, D., & Malenka, R. (1992). The influence of prior synaptic activity on the induction of long-term potentiation. *Science*, 255(5045), 730-733.
- Jarrard, L. E. (1993). On the role of the hippocampus in learning and memory in the rat. *Behavioral and Neural Biology*, 60(1), 9-26.
- Jeffery, K. J., & Morris, R. G. (1993). Cumulative long-term potentiation in the rat dentate gyrus correlates with, but does not modify, performance in the water maze. *Hippocampus*, 3(2), 133-140.
- Johnston, D., & Amaral, D. G. (1998). Hippocampus. In *The Synaptic Organization of the Brain* (pp. 417-458). New York: Oxford University Press.

- Kager, H., Wadman, W.J., & Somjen, G. G. (2006). Seizure-like afterdischarges simulated in a model neuron. *Journal of Computational Neuroscience*, 22(2), 105-128.
- Kaibara, T., & Leung, L. (1993). Basal versus apical dendritic long-term potentiation of commissural afferents to hippocampal CA1: A current-source density study. *The Journal of Neuroscience*, 13(6), 2391-2404.
- Kandel, E., & Spencer, W. (1961). Excitation and inhibition of single pyramidal cells during hippocampal seizure. *Experimental Neurology*, 4(2), 162-179.
- Kandel, E. R., Schwartz, J. H., Jessell, T. M., Siegelbaum, S. A., & Hudspeth, A. J. (2014). *Principles of neural science*. NY, NY: McGraw-Hill Medical.
- Krishnan, G. P., & Bazhenov, M. (2011). Ionic Dynamics Mediate Spontaneous Termination of Seizures and Postictal Depression State. *Journal of Neuroscience*, 31(24), 8870-8882.
- Leão, R. N., Mikulovic, S., Leão, K. E., Munguba, H., Gezelius, H., Enjin, A.,... Kullander, K. (2012). OLM interneurons differentially modulate CA3 and entorhinal inputs to hippocampal CA1 neurons. *Nature Neuroscience*, 15(11), 1524-1530.
- Leung, L.S., & Shen, B. (1993). Long-Term Potentiation in Hippocampal CA1: Effects of Afterdischarges, NMDA Antagonists, and Anticonvulsants. *Experimental Neurology*, 119(2), 205-214.
- Leung, L. S., & Shen, B. (1995). Long-term potentiation at the apical and basal dendritic synapses of CA1 after local stimulation in behaving rats. *Journal of Neurophysiology*, 73(5), 1938-1946.
- Leung, L. S., & Wu, C. (2003). Kindling suppresses primed-burst-induced long-term potentiation in hippocampal CA1. *NeuroReport*, 14(2), 211-214.
- Leung, L. S. (2010). Field Potential Generation and Current Source Density Analysis. In: *Electrophysiological Recording Techniques*, Vertes, R.P. & Stackman, R.W, (Eds.), Humana Press, Clifton, N.J., NeuroMethods Volume 54:1-26.
- Li, S., Cullen, W. K., Anwyl, R., & Rowan, M. J. (2003). Dopamine-dependent facilitation of LTP induction in hippocampal CA1 by exposure to spatial novelty. *Nature Neuroscience*, 6(5), 526-531.
- Lynch, G., Larson, J., Kelso, S., Barrionuevo, G., & Schottler, F. (1983). Intracellular injections of EGTA block induction of hippocampal long-term potentiation. *Nature*, 305(5936), 719-721.
- Lynch, M. A. (2004). Long-Term Potentiation and Memory. *Physiological Reviews*, 84(1), 87-136.

- Maruki, K., Izaki, Y., Nomura, M., & Yamauchi, T. (2001). Differences in paired-pulse facilitation and long-term potentiation between dorsal and ventral CA1 regions in anesthetized rats. *Hippocampus*, *11*(6), 655-661.
- Mayford, M., Bach, M. E., Huang, Y., Wang, L., Hawkins, R. D., & Kandel, E. R. (1996). Control of Memory Formation Through Regulated Expression of a CaMKII Transgene. *Science*, *274*(5293), 1678-1683.
- Megías, M., Emri, Z., Freund, T., & Gulyás, A. (2001). Total number and distribution of inhibitory and excitatory synapses on hippocampal CA1 pyramidal cells. *Neuroscience*, *102*(3), 527-540.
- Moore, S. D., Barr, D. S., & Wilson, W. A. (1993). Seizure-like activity disrupts LTP in vitro. *Neuroscience Letters*, *163*(1), 117-119.
- Morris, R. G. (2003). Long-term potentiation and memory. *Royal Society*, *358*(1432), 643-647.
- Morris, R., Anderson, E., Lynch, G. S. G., Baudry, M., Anderson, A., Baudry, B. (1986). Selective impairment of learning and blockade of long term potentiation by an N-methyl-D-aspartate receptor antagonist, APV-5. *Nature*, *319*(6056), 774-776.
- Moser, E. I., Krobot, K. A., Moser, M., & Morris, R. G. (1998). Impaired Spatial Learning after Saturation of Long-Term Potentiation. *Science*, *281*(5385), 2038-2042.
- Navakkode, S., Sajikumar, S., Korte, M., & Soong, T. W. (2012). Dopamine induces LTP differentially in apical and basal dendrites through BDNF and voltage-dependent calcium channels. *Learning & Memory*, *19*(7), 294-299.
- Nogami, T., Beppu, H., Tokoro, T., Moriguchi, S., Shioda, N., Fukunaga, K., . . . Kitajima, I. (2010). Reduced expression of the ATRX gene, a chromatin-remodeling factor, causes hippocampal dysfunction in mice. *Hippocampus*, *21*(6), 678-687.
- O'Keefe, J. (1979). A review of the hippocampal place cells. *Progress in Neurobiology*, *13*(4), 419-439.
- Perlin, J. B., Churn, S. B., Lothman, E. W., & Delorenzo, R. J. (1992). Loss of type II calcium/calmodulin-dependent kinase activity correlates with stages of development of electrographic seizures in status epilepticus in rat. *Epilepsy Research*, *11*(2), 111-118.
- Rossato, J. I., Bevilaqua, L. R., Izquierdo, I., Medina, J. H., & Cammarota, M. (2009). Dopamine Controls Persistence of Long-Term Memory Storage. *Science*, *325*(5943), 1017-1020.
- Sajikumar, S., & Frey, J. U. (2004). Late-associativity, synaptic tagging, and the role of dopamine during LTP and LTD. *Neurobiology of Learning and Memory*, *82*(1), 12-25.
- Satoshi, F., Yoichiro, K., Masami, M., Hidekazu, F., Hiroshi, S., Kenya, K., . . . Hiroshi, K. (1996).

- The long-term suppressive effect of prior activation of synaptic inputs by low-frequency stimulation on induction of long-term potentiation in CA1 neurons of guinea pig hippocampal slices. *Experimental Brain Research*, 111(3).
- Schulz, P., Cook, E., & Johnston, D. (1994). Changes in paired-pulse facilitation suggest presynaptic involvement in long-term potentiation. *The Journal of Neuroscience*, 14(9), 5325-5337.
- Scoville, W. B., & Milner, B. (1957). Loss of recent memory after bilateral hippocampal lesions. *Journal of Neurology, Neurosurgery & Psychiatry*, 20(1), 11-21.
- Somjen, G. G., Aitken, P. G., Giacchino, J. L., & Mcnamara, J. O. (1985). Sustained potential shifts and paroxysmal discharges in hippocampal formation. *Journal of Neurophysiology*, 53(4), 1079-1097.
- Stasheff, S. F., Bragdon, A. C., & Wilson, W. A. (1985). Induction of epileptiform activity in hippocampal slices by trains of electrical stimuli. *Brain Research*, 344(2), 296-302.
- Stasheff, S., Anderson, W., Clark, S., & Wilson, W. (1989). NMDA antagonists differentiate epileptogenesis from seizure expression in an in vitro model. *Science*, 245(4918), 648-651.
- Stretton, J., & Thompson, P. (2012). Frontal lobe function in temporal lobe epilepsy. *Epilepsy Research*, 98(1), 1-13.
- Sutherland, R. J., Dringenberg, H. C., & Hoelsing, J. M. (1993). Induction of long-term potentiation at perforant path dentate synapses does not affect place learning or memory. *Hippocampus*, 3(2), 141-147.
- Suárez, L. M., Cid, E., Gal, B., Inostroza, M., Brotons-Mas, J. R., Gómez-Domínguez, D., . . . Solís, J. M. (2012). Systemic Injection of Kainic Acid Differently Affects LTP Magnitude Depending on its Epileptogenic Efficiency. *PLoS ONE*, 7(10).
- Tatum, W.O. (2012). Mesial Temporal Lobe Epilepsy. *Journal of Clinical Neurophysiology*, 29(5), 356-365.
- Twele, F., Schidlitzki, A., Töllner, K., & Löscher, W. (2017). The intrahippocampal kainate mouse model of mesial temporal lobe epilepsy: Lack of electrographic seizure-like events in sham controls. *Epilepsia Open*, 2(2), 180-187.
- Woo, N. H., & Nguyen, P. V. (2002). "Silent" Metaplasticity of the Late Phase of Long-Term Potentiation Requires Protein Phosphatases. *Learning & Memory*, 9(4), 202-213.
- Wu, K., & Leung, L. (2003). Increased dendritic excitability in hippocampal CA1 in vivo in the kainic acid model of temporal lobe epilepsy: a study using current source density analysis. *Neuroscience*, 116(2), 599-616.

Zhou, C., Bell, J. J., Sun, H., & Jensen, F. E. (2011). Hypoxia-Induced Neonatal Seizures Diminish Silent Synapses and Long-Term Potentiation in Hippocampal CA1 Neurons. *Journal of Neuroscience*, *31*(50), 18211-18222.

Zucker, R. S., & Regehr, W. G. (2002). Short-term Synaptic Plasticity. *Annual Review Physiology*, *64*, 355-405.

APPENDIX**Ethical Approval for Animal Use**

PI Name: Leung, Stan (lai-wo)

AUP Number: 2010-261

AUP Title: Neural plasticity of the forebrain

Yearly Renewal Date: 04/01/2017

The YEARLY RENEWAL to Animal Use Protocol (AUP) 2010-261 has been approved, and will be approved for one year following the above review date.

The holder of this Animal Use Protocol is responsible to ensure that all associated safety components (biosafety, radiation safety, general laboratory safety) comply with institutional safety standards and have received all necessary approvals. Please consult directly with your institutional safety officers.

Submitted by: Schoelier, Marianne on behalf of the Animal Use Subcommittee

APPENDIX

Copyright Permission

License Number	4414520477203
License date	Aug 22, 2018
Licensed Content Publisher	Elsevier
Licensed Content Publication	Neuroscience
Licensed Content Title	Total number and distribution of inhibitory and excitatory synapses on hippocampal CA1 pyramidal cells
Licensed Content Author	M Megías,Zs Emri,T.F Freund,A.I Gulyás
Licensed Content Date	Feb 5, 2001
Licensed Content Volume	102
Licensed Content Issue	3
Licensed Content Pages	14
Start Page	527
End Page	540
Type of Use	reuse in a thesis/dissertation
Portion	figures/tables/illustrations
Number of figures/tables/illustrations	1
Format	electronic
Are you the author of this Elsevier article?	No
Will you be translating?	No
Original figure numbers	Fig 2
Title of your thesis/dissertation	The effect of Seizure (Afterdischarge) on Hippocampal LTP
Expected completion date	Sep 2018
Estimated size (number of pages)	86
Requestor Location	University of Western Ontario 1151 Richmond St London, ON N6A 3K7 Canada Attn: University of Western Ontario

CURRICULUM VITAE

Name: Vishaka Dinesh Rajan

**Post-secondary
Education and
Degrees:** University of Toronto
Toronto, Ontario, Canada
2012-2016, Honours B.Sc.
Human Biology and Psychology

University of Western Ontario
London, Ontario, Canada
2016-2018, M.Sc.
Neuroscience

**Related Work
Experience:** Teaching Assistant
University of Western Ontario
2016-2018
Neuroscience 9500

Poster Presentation

Rajan V, Leung LS (2018) The effects of a single afterdischarge on long-term potentiation in the mouse hippocampus. Southwestern Ontario Neuroscience Association (SONA) meeting at the University of Guelph.